Status of Multi-lepton anomalies at the LHC and its implications

Bruce Mellado

The Wits Institute for Collider Particle Physics and iThemba LABS

Institute for Collider Particle Physics
University of the Witwatersrand

NRF National Research Foundation
iThemba LABS Laboratory for Accelerator Based Sciences

IAS High Energy Physics, Hong Kong, 21/01/21

Outline

- The simplified model
- The multilepton problem
  - Methodology
  - The anatomy of the anomalies
- Impact on Higgs physics
- The Muon g-2
- Leptophilic excesses in astrophysics
  - The MeerKat/SKA

The Simplified Model and 2HDM+S

Eur. Phys. J. C (2016) 76:580

The simplified Model (from Run I)

1. **The starting point of the hypothesis is the existence of a boson, H, that contains Higgs-like interactions, with a mass in the range 250-280 GeV**
2. **In order to avoid large quartic couplings, incorporate a mediator scalar, S, that interacts with the SM and Dark Matter.**
3. **Dominance of H→Sh,SS decay over other decays**

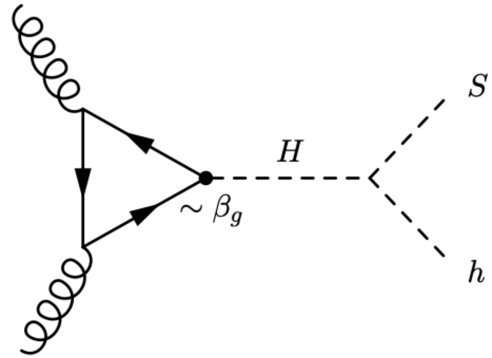

(a) Gluon fusion (ggF).

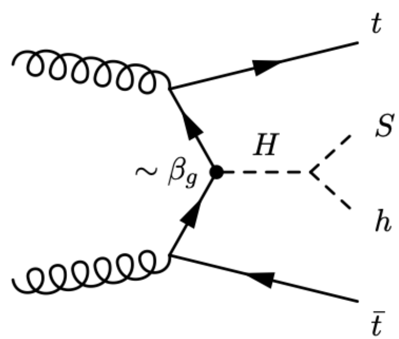

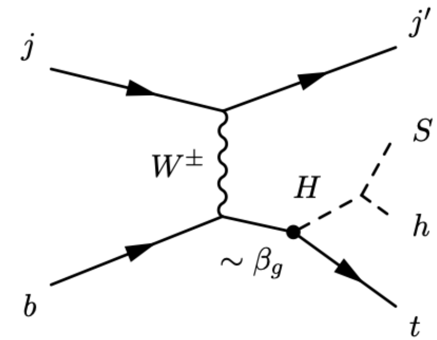

$$\mathcal{L}_{\rm int} \supset -\beta_g \frac{m_t}{v} t\bar{t}H + \beta_V \frac{m_V^2}{v} g_{\mu\nu}\, V^\mu V^\nu H$$

$$\mathcal{L}_{HhS} = -\frac{1}{2}\, v\Big[\lambda_{hhS} hhS + \lambda_{hSS} hSS + \lambda_{HHS} HHS + \lambda_{HSS} HSS + \lambda_{HhS} HhS\Big],$$

The Lagrangian

Can be embedded into 2HDM+S (N2HDM)
See also M.Muhlleitner et al.
arXiv:1612.01309
arXiv:1708.01578

$$\mathcal{L}_K = \frac{1}{2}\partial_\mu S \partial^\mu S - \frac{1}{2} m_S^2 SS,$$

$$\mathcal{L}_{SVV'} = \frac{1}{4}\kappa_{_{Sgg}} \frac{\alpha_s}{12\pi v} S G^{a\mu\nu} G^a_{\mu\nu} + \frac{1}{4}\kappa_{_{S\gamma\gamma}} \frac{\alpha}{\pi v} S F^{\mu\nu} F_{\mu\nu} + \frac{1}{4}\kappa_{_{SZZ}} \frac{\alpha}{\pi v} S Z^{\mu\nu} Z_{\mu\nu} + \frac{1}{4}\kappa_{_{SZ\gamma}} \frac{\alpha}{\pi v} S Z^{\mu\nu} F_{\mu\nu} + \frac{1}{4}\kappa_{_{SWW}} \frac{2\alpha}{\pi s_w^2 v} S W^{+\mu\nu} W^-_{\mu\nu},$$

$$\mathcal{L}_{Sf\bar{f}} = -\sum_f \kappa_{_{Sf}} \frac{m_f}{v} S \bar{f} f,$$

$$\mathcal{L}_{HhS} = -\frac{1}{2}\, v \left[\lambda_{_{hhS}} hhS + \lambda_{_{hSS}} hSS + \lambda_{_{HHS}} HHS + \lambda_{_{HSS}} HSS + \lambda_{_{HhS}} HhS \right],$$

$$\mathcal{L}_{S\chi} = -\frac{1}{2}\, v\, \lambda_{_{S\chi\chi}} S\chi\chi - \frac{1}{2}\lambda_{_{SS\chi\chi}} SS\chi\chi.$$

$$\mathcal{L}_S = \mathcal{L}_K + \mathcal{L}_{SVV'} + \mathcal{L}_{Sf\bar{f}} + \mathcal{L}_{hHS} + \mathcal{L}_{S\chi}$$

Note that some of the effective quartic couplings shown earlier appear here as trilinear.
What was formerly a three body decay is now a two body decay.

The Decays of H

- In the general case, H can have couplings as those displayed by a Higgs boson in addition to decays involving the intermediate scalar and Dark Matter

$$H \to WW, ZZ, q\bar{q}, gg, Z\gamma, \gamma\gamma, \chi\chi$$

$$+ \quad H \to SS, Sh, hh$$

Dominant decays

Diboson decay

$$H \to h(+X), S(+X)$$

The 2HDM+S

Eur. Phys. J. C (2016) 76:580

Introduce singlet real scalar, S.

2HDM potential, $\mathscr{V}(\Phi_1, \Phi_2)$

$$= m_1^2 \Phi_1^\dagger \Phi_1 + m_2^2 \Phi_2^\dagger \Phi_2 - m_{12}^2 \left(\Phi_1^\dagger \Phi_2 + \text{h.c.} \right)$$
$$+ \frac{1}{2}\lambda_1 \left(\Phi_1^\dagger \Phi_1 \right)^2 + \frac{1}{2}\lambda_2 \left(\Phi_2^\dagger \Phi_2 \right)^2$$
$$+ \lambda_3 \left(\Phi_1^\dagger \Phi_1 \right) \left(\Phi_2^\dagger \Phi_2 \right) + \lambda_4 \left| \Phi_1^\dagger \Phi_2 \right|^2$$
$$+ \frac{1}{2}\lambda_5 \left[\left(\Phi_1^\dagger \Phi_2 \right)^2 + \text{h.c.} \right]$$
$$+ \left\{ \left[\lambda_6 \left(\Phi_1^\dagger \Phi_1 \right) + \lambda_7 \left(\Phi_2^\dagger \Phi_2 \right) \right] \Phi_1^\dagger \Phi_2 + \text{h.c.} \right\}$$

2HDM+S potential

$$\mathscr{V}(\Phi_1, \Phi_2) + \frac{1}{2} m_{S_0}^2 S^2 + \frac{\lambda_{S_1}}{2} \Phi_1^\dagger \Phi_1 S^2$$
$$+ \frac{\lambda_{S_2}}{2} \Phi_2^\dagger \Phi_2 S^2 + \frac{\lambda_{S_3}}{4} (\Phi_1^\dagger \Phi_2 + \text{h.c}) S^2$$
$$+ \frac{\lambda_{S_4}}{4!} S^4 + \mu_1 \Phi_1^\dagger \Phi_1 S + \mu_2 \Phi_2^\dagger \Phi_2 S$$
$$+ \mu_3 \left[\Phi_1^\dagger \Phi_2 + \text{h.c} \right] S + \mu_S S^3 .$$

Out of considerations of simplicity, assume S to be Higgs-like, which is not too far fetched.

The model leads to rich phenomenology. ***Of particular interest are multilepton signatures***

S. No.	Scalars	Decay modes
D.1	h	$b\bar{b}$, $\tau^+\tau^-$, $\mu^+\mu^-$, $s\bar{s}$, $c\bar{c}$, gg, $\gamma\gamma$, $Z\gamma$, W^+W^-, ZZ
D.2	H	D.1, hh, SS, Sh
D.3	A	D.1, $t\bar{t}$, Zh, ZH, ZS, $W^{\pm}H^{\mp}$
D.4	$H^{\pm}$	$W^{\pm}h$, $W^{\pm}H$, $W^{\pm}S$
D.5	S	D.1, $\chi\chi$

arXiv:1606.01674

Scalar	Production mode	Search channels
H	$gg \to H, Hjj$ (ggF and VBF)	Direct SM decays as in Table 1 $\to SS/Sh \to 4W \to 4\ell + E_T^{miss}$ $\to hh \to \gamma\gamma b\bar{b}$, $b\bar{b}\tau\tau$, $4b$, $\gamma\gamma WW$ etc. $\to Sh$ where $S \to \chi\chi \implies \gamma\gamma$, $b\bar{b}$, $4\ell + E_T^{miss}$
	$pp \to Z(W^{\pm})H$ ($H \to SS/Sh$)	$\to 6(5)l + E_T^{miss}$ $\to 4(3)l + 2j + E_T^{miss}$ $\to 2(1)l + 4j + E_T^{miss}$
	$pp \to t\bar{t}H, (t+\bar{t})H$ ($H \to SS/Sh$)	$\to 2W + 2Z + E_T^{miss}$ and b-jets $\to 6W \to 3$ same sign leptons + jets and E_T^{miss}
$H^{\pm}$	$pp \to tH^{\pm}$ ($H^{\pm} \to W^{\pm}H$)	$\to 6W \to 3$ same sign leptons + jets and E_T^{miss}
	$pp \to tbH^{\pm}$ ($H^{\pm} \to W^{\pm}H$)	Same as above with extra b-jet
	$pp \to H^{\pm}H^{\mp}$ ($H^{\pm} \to HW^{\pm}$)	$\to 6W \to 3$ same sign leptons + jets and E_T^{miss}
	$pp \to H^{\pm}W^{\pm}$ ($H^{\pm} \to HW^{\pm}$)	$\to 6W \to 3$ same sign leptons + jets and E_T^{miss}
A	$gg \to A$ (ggF)	$\to t\bar{t}$ $\to \gamma\gamma$
	$gg \to A \to ZH$ ($H \to SS/Sh$)	Same as $pp \to ZH$ above, but with resonance structure over final state objects
	$gg \to A \to W^{\pm}H^{\mp}(H^{\mp} \to W^{\mp}H)$	$6W$ signature with resonance structure over final state objects

Multi-lepton final states

It is paramount to remark that the excesses are seen in final states that were predicted 2015/2016 on the basis of a simplified model and not the result of scan of the available phase-space. Additionally, the parameters of the model where fixed then leaving only one degree of freedom: normalization Thus, no look-elsewhere effects in parameter or phase-space

$$pp \to H \to Sh$$
$$\to \ell^+\ell^- + X$$

Expect di-leptons (m_{ll}<100 GeV) with jets and b-jets with rates comparable to that of the SM Higgs boson

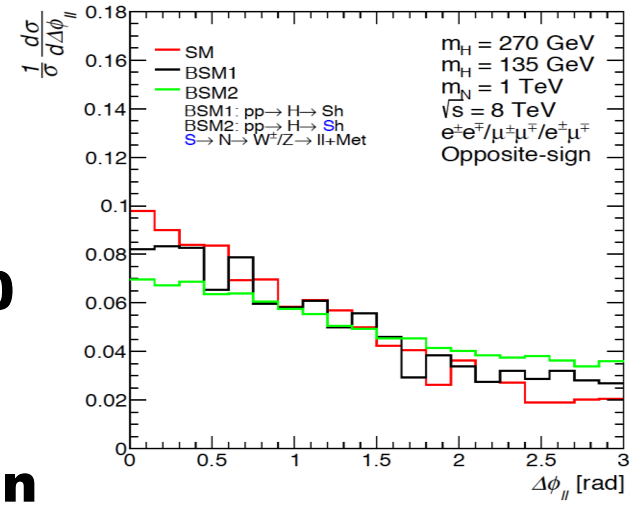

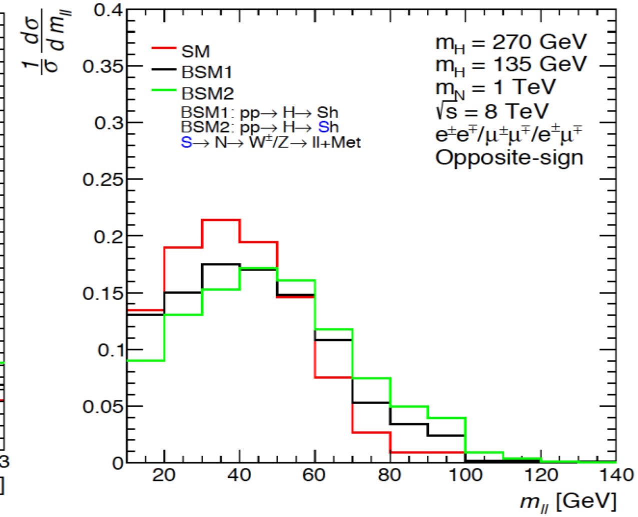

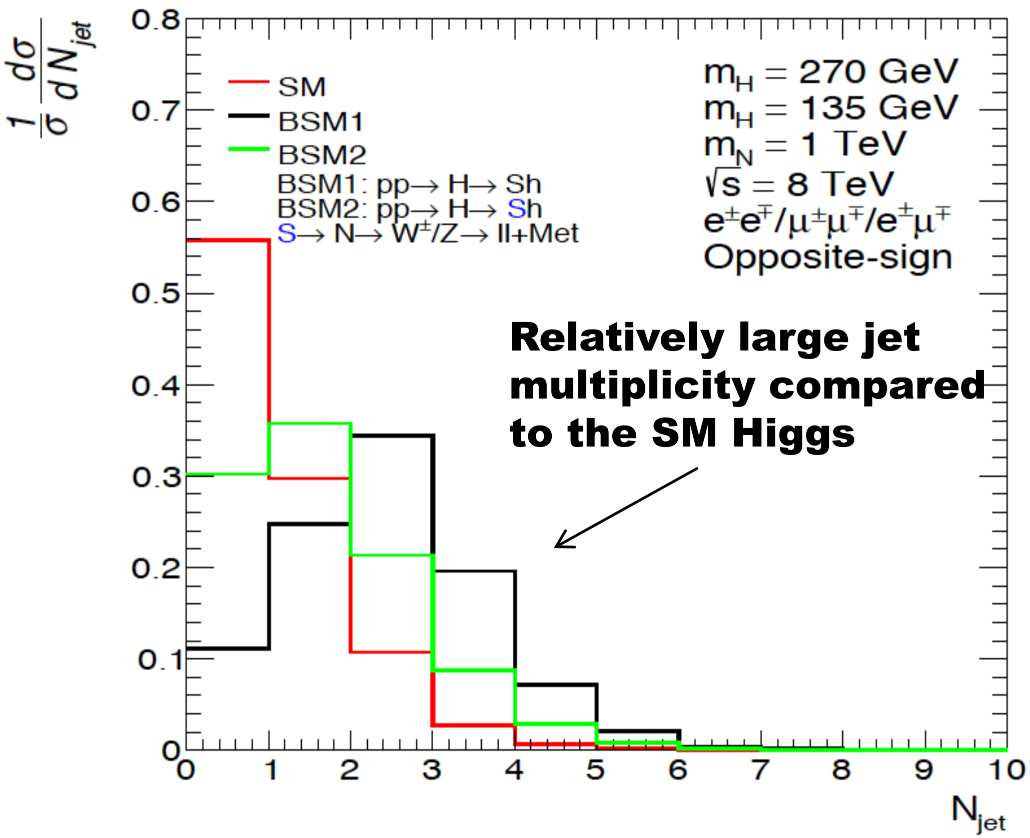

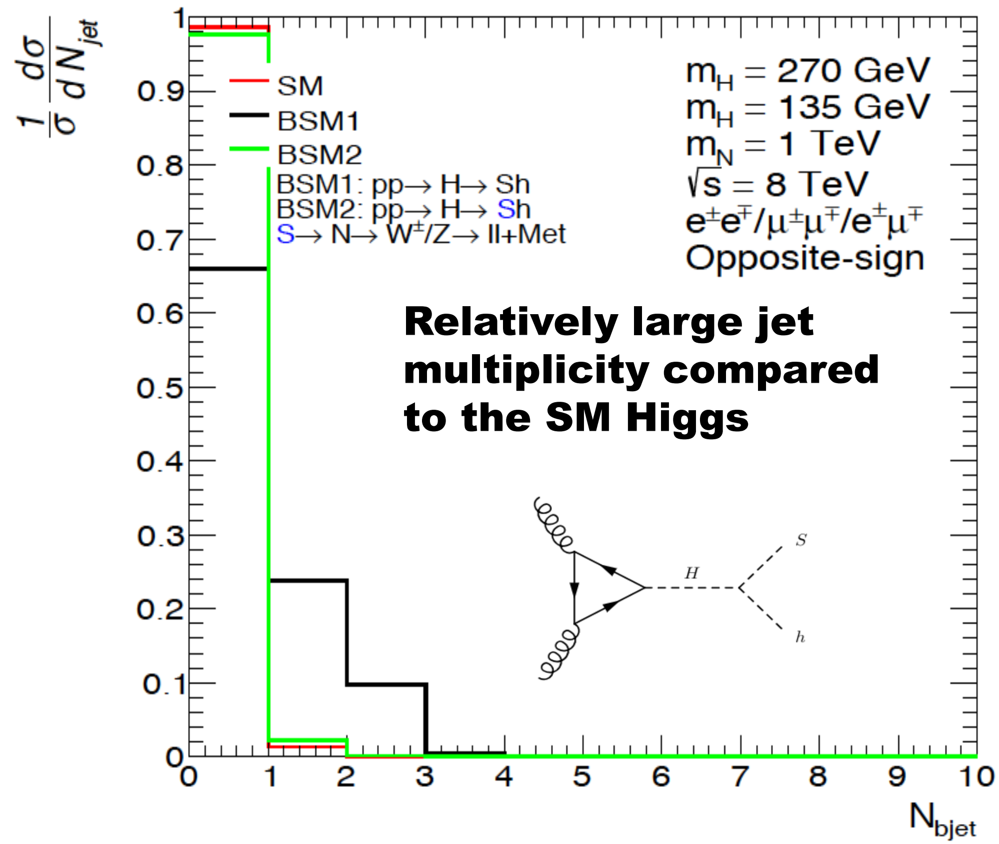

Top associated Higgs production
(Multi-lepton final states)

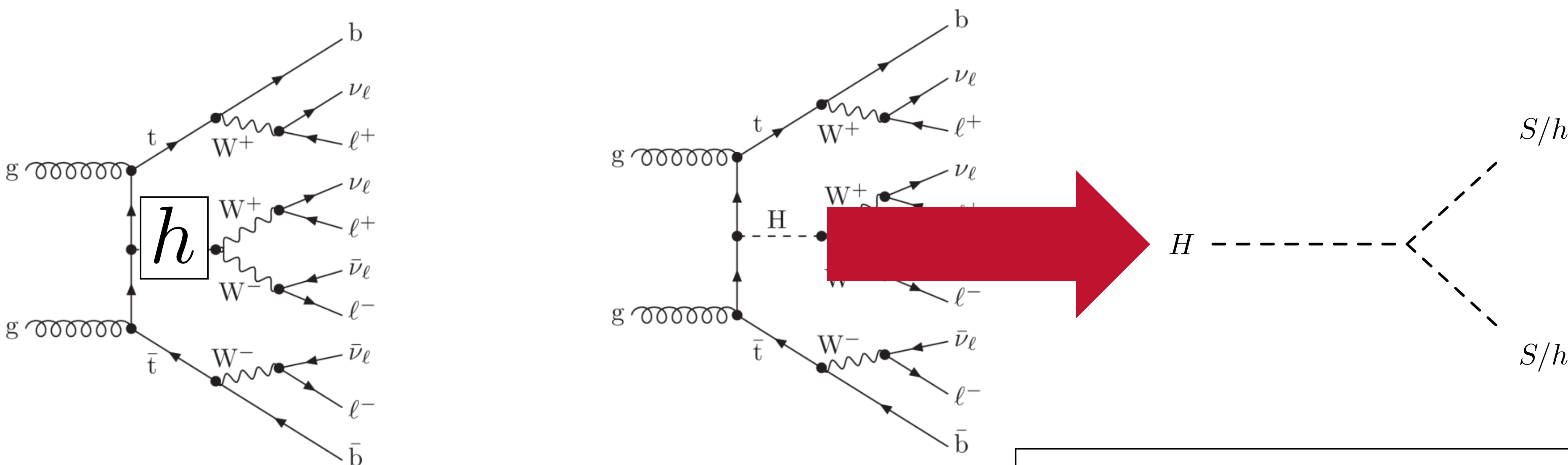

Reduced cross-section of ttH+tH is compensated by di-boson, (SS, Sh) decay and large Br(S→WW). Production of same sign leptons, three leptons is enhanced. Enhanced tH cross-section

Produces SS 2l, 3l with b-jets, including 3 b-jets

Explains anomalously large ttW+tth cross-sections seen by ATLAS and CMS

Methodology

(to avoid biases and look-else-where effects)

Based Higgs p_T, hh, tth, VV in Run 1
Eur. Phys. J. C (2016) 76:580

Model defined and predictions made for multilepton excesses

Multi-lepton excesses in Run 1 and few Run 2 results available in 2017

J.Phys.G 45 (2018) 11, 115003

Model <u>parameters fixed in 2017</u> with m_H=270 GeV, m_S=150 GeV, S treated as SM Higgs-like, dominance of H→Sh,SS

Fixed final states and phase-space defined by fixed model parameters.
<u>NO tuning, NO scanning</u>

Study same results with more data in Run 2

Study new final states where excesses predicted and data available in Run 1 and Run 2 (e.g., SS0b, 3l0b, ZW)

J.Phys. G46 (2019) no.11, 115001
JHEP 1910 (2019) 157
Chin.Phys.C 44 (2020) 6, 063103
Physics Letters B 811 (2020) 135964
arXiv:1912.00699

BSM inputs to the fit

- **The following <u>assumptions</u> are made:**
  - a. The masses of H and S are fixed to $m_H = 270$ GeV and $m_S = 150$ GeV
  - b. The only significant production mechanisms of H come from the t-t-H Yukawa coupling:
    - Gluon fusion
    - Top associated production
  - c. The Yukawa coupling is scaled away from the SM Higgs-like value by the free parameter β_g
  - d. The BR of $H \rightarrow Sh$ is fixed to 100%
  - e. The BRs of S are Higgs-like
- **Therefore, the only free parameter in the fits is β_g^2**

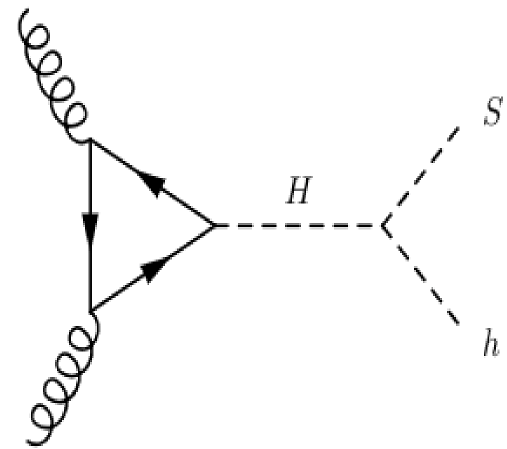

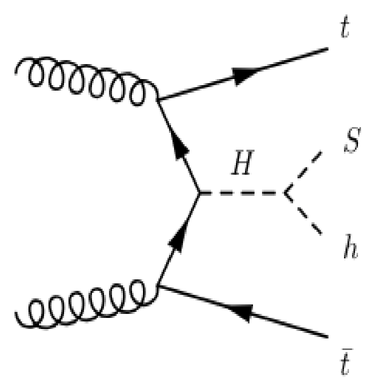

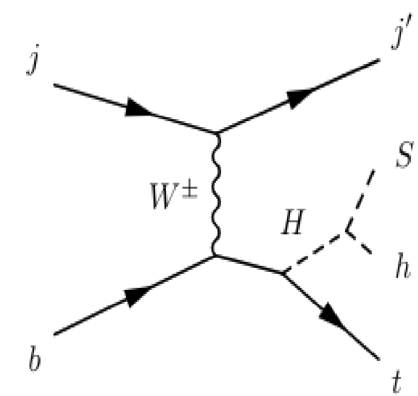

Selection	Best-fit β_g^2	Significance
ATLAS Run 1 SS $\ell\ell$ and $\ell\ell\ell + b$-jets	6.51 ± 2.99	2.37σ
ATLAS Run 1 OS $e\mu + b$-jets	4.09 ± 1.37	2.99σ
CMS Run 2 SS $e\mu$, $\mu\mu$ and $\ell\ell\ell + b$-jets	1.41 ± 0.80	1.75σ
CMS Run 2 OS $e\mu$	2.79 ± 0.52	5.45σ
CMS Run 2 $\ell\ell\ell + E_{\mathrm{T}}^{\mathrm{miss}}$ (WZ)	9.70 ± 3.88	2.36σ
ATLAS Run 2 SS $\ell\ell$ and $\ell\ell\ell + b$-jets	2.22 ± 1.19	2.01σ
ATLAS Run 2 OS $e\mu + b$-jets	5.42 ± 1.28	4.06σ
ATLAS Run 2 $\ell\ell\ell + E_{\mathrm{T}}^{\mathrm{miss}}$ (WZ)	9.05 ± 3.35	2.52σ
Combination	2.92 ± 0.35	8.04σ

The simplidied model seems to describe the discrepancies in different corners of the phase-space with large differences in cross-sections, eg, OS and SS di-leptons

Combination of fit results

- **Simultaneous fit for all measurements:**
- **To the right: (-2 log) profile likelihood ratio for each individual result and the combination of them all**
- **The significance for each fit is calculated as**

$$\sqrt{-2\log\lambda(0)}$$

- **Best-fit: $\beta_g^2 = 2.92 \pm 0.35$**
- **Corresponds to 8.04σ**

Excesses have been growing since. See backup slides

JHEP 1910 (2019) 157

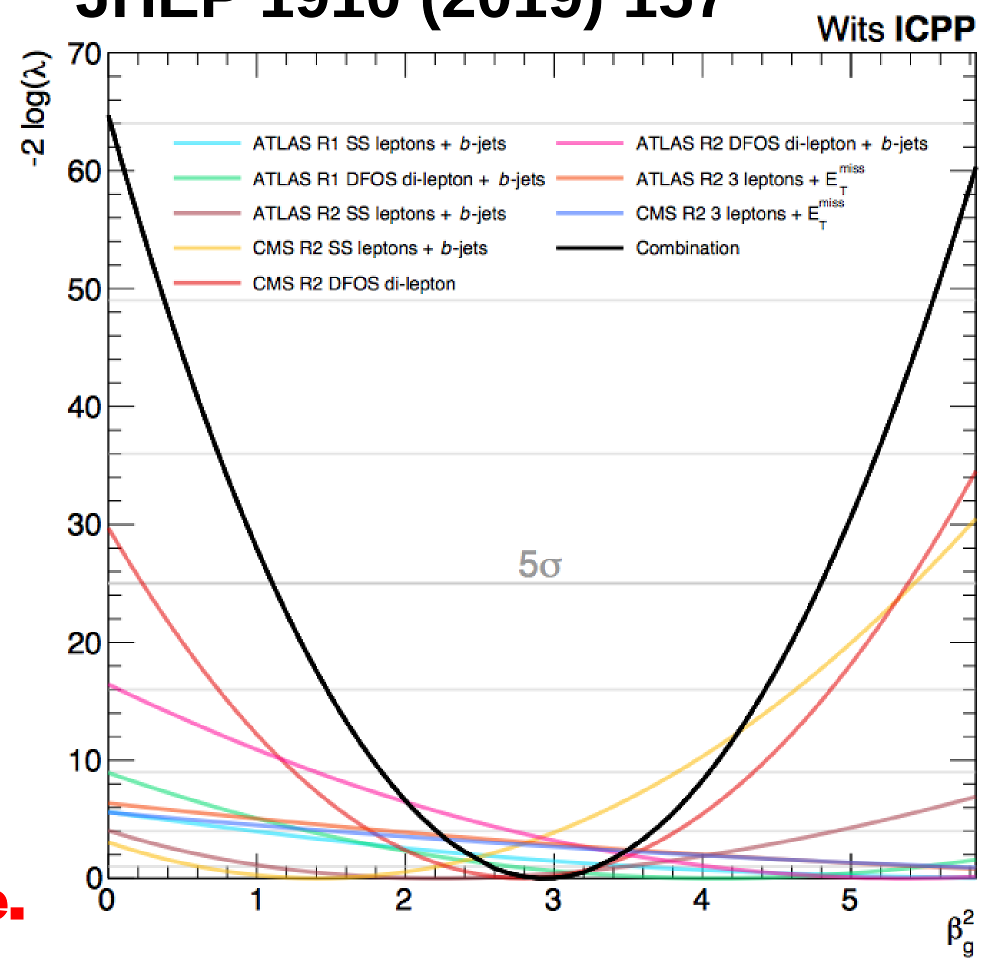

Interpretation: Measure of the inability of current MC tools to describe multiple-lepton data and how a simplified model with H→Sh is able to capture the effect with one parameter

The anatomy of inclusive ttW at the LHC

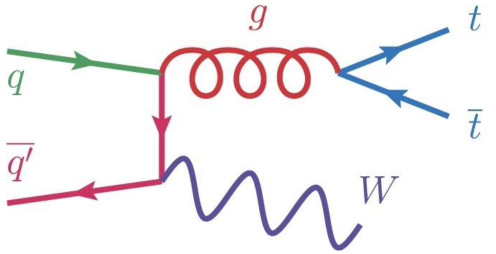

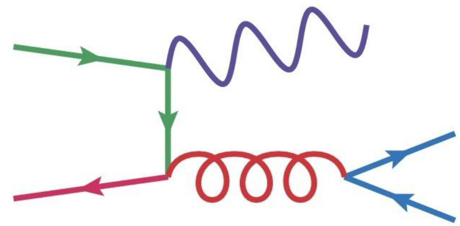

S.Buddenbrock, R.Ruiz and B.M.

Physics Letters B 811 (2020) 135964

Using fixed order computations at $\mathcal{O}(\alpha_s^4\alpha)$ and NLO multi-jet matching yielding similar (10%-14%) corrections to the inclusive rate

$i\,j \to t\,\bar{t}\,W^{\pm}\,k\,l$						
(i,j)	(k,l)	$p_T^{j_1\ \min}$	$p_T^{j_2\ \min}$	σ [fb]	$\pm\delta_{\mu_f,\mu_r}$	$\pm\delta_{\rm PDF}$
All	All	75 GeV	75 GeV	34.7 (100%)	$^{+57\%}_{-34\%}$	$^{+1.1\%}_{-1.1\%}$
(g,Q)	(g,Q)			23.7 (68%)		
(Q,Q)	(Q,Q)			6.99 (20%)		
(Q,Q)	(g,g)			3.63 (10%)		
(g,g)	$(q,\bar{q})$			0.437 (1.3%)		
All	All	100 GeV	75 GeV	33.1 (100%)	$^{+57\%}_{-34\%}$	$^{+1.0\%}_{-1.0\%}$
(g,Q)	(g,Q)			22.6 (68 %)		
(Q,Q)	(Q,Q)			6.78 (20%)		
(Q,Q)	(g,g)			3.28 (9.9%)		
(g,g)	$(q,\bar{q})$			0.409 (1.2%)		
All	All	100 GeV	100 GeV	21.2 (100%)	$^{+57\%}_{-34\%}$	$^{+1.1\%}_{-1.1\%}$
(g,Q)	(g,Q)			14.3 (67%)		
(Q,Q)	(Q,Q)			4.91 (23%)		
(Q,Q)	(g,g)			1.75 (8%)		
(g,g)	$(q,\bar{q})$			2.58 (1%)		
(g,q_V)	(g,q_V)	75 GeV	75 GeV	20.1 (58%)	$^{+58\%}_{-35\%}$	$^{+2.3\%}_{-2.3\%}$
(g,q_V)	(g,q_V)	100 GeV	75 GeV	19.3 (58%)	$^{+58\%}_{-35\%}$	$^{+2.3\%}_{-2.3\%}$
(g,q_V)	(g,q_V)	100 GeV	100 GeV	12.2 (58%)	$^{+59\%}_{-35\%}$	$^{+2.4\%}_{-2.4\%}$

Table 2: Total cross sections [fb] at $\sqrt{s}$ = 13 TeV for the $pp \to t\bar{t}W^{\pm}jj$ process at LO, with scale and PDF uncertainties [%], for representative $p_T^{j_k\ \min}$ with $|\eta^j| < 4.0$. Also shown is the decomposition according to partonic channel, for $q_V \in \{u,d\}$, $q \in \{u,d,c,s\}$, and $Q \in \{q,\bar{q}\}$.

Detailed studies that include the decomposition in partonic channels and differential distributions

Tension between data and predictions does not wane.
For this process a complete NNLO computation is needed to reduce theory uncertainty

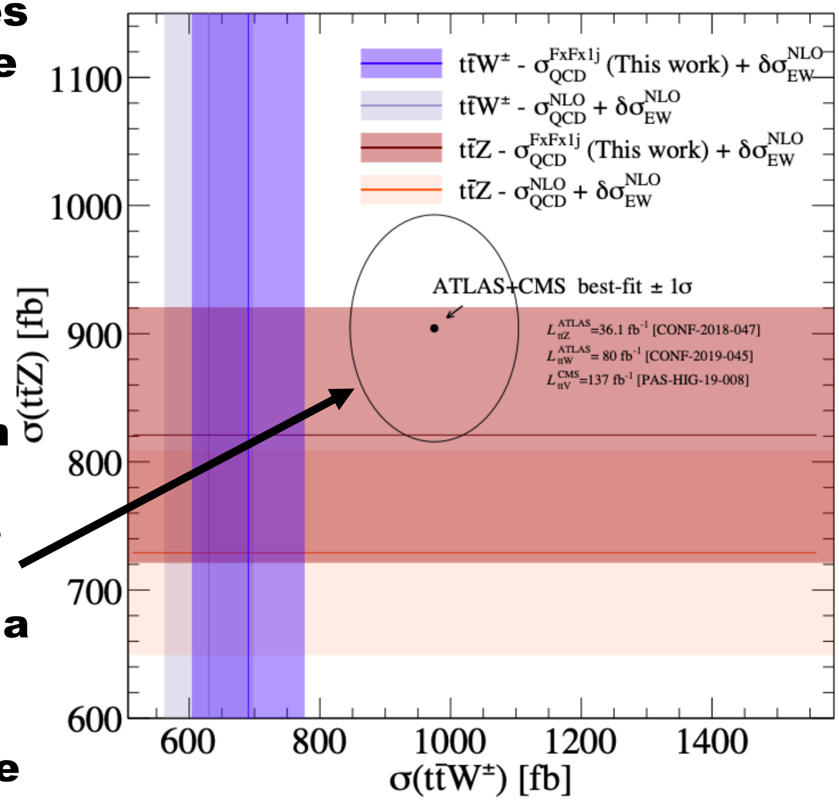

Anatomy of the multi-lepton anomalies

JHEP 1910 (2019) 157

Final state	Characteristic	Dominant SM process
l^+l^- + jets, b-jets	m_{ll}<100 GeV, dominated by 0b-jet and 1b-jet	tt+Wt
l^+l^- + full-jet veto	m_{ll}<100 GeV	WW
$l^\pm l^\pm$ + b-jets	Excess with $N_\pm$>2, moderate H_T	ttV
$l^\pm l^\pm l$ + b-jets	Moderate H_T	ttV
Z(→l^+l^-)+l	p_{TZ}<100 GeV	ZW

Anomalies cannot be explained by mismodelling of a particular process, e.g. ttbar production alone

Impact on Higgs Physics

The presence of a BSM signal of the type H→Sh would lead to:

- **The presence of extra leptons in association with h. Affects the Wh measurement (arXiv:1912.00699)**
- **Distortion of Higgs p_T and rapidity (under study)**

No tuning of model parameters performed. Look at fixed corners of the phase-space fixed with parameters of 2017.

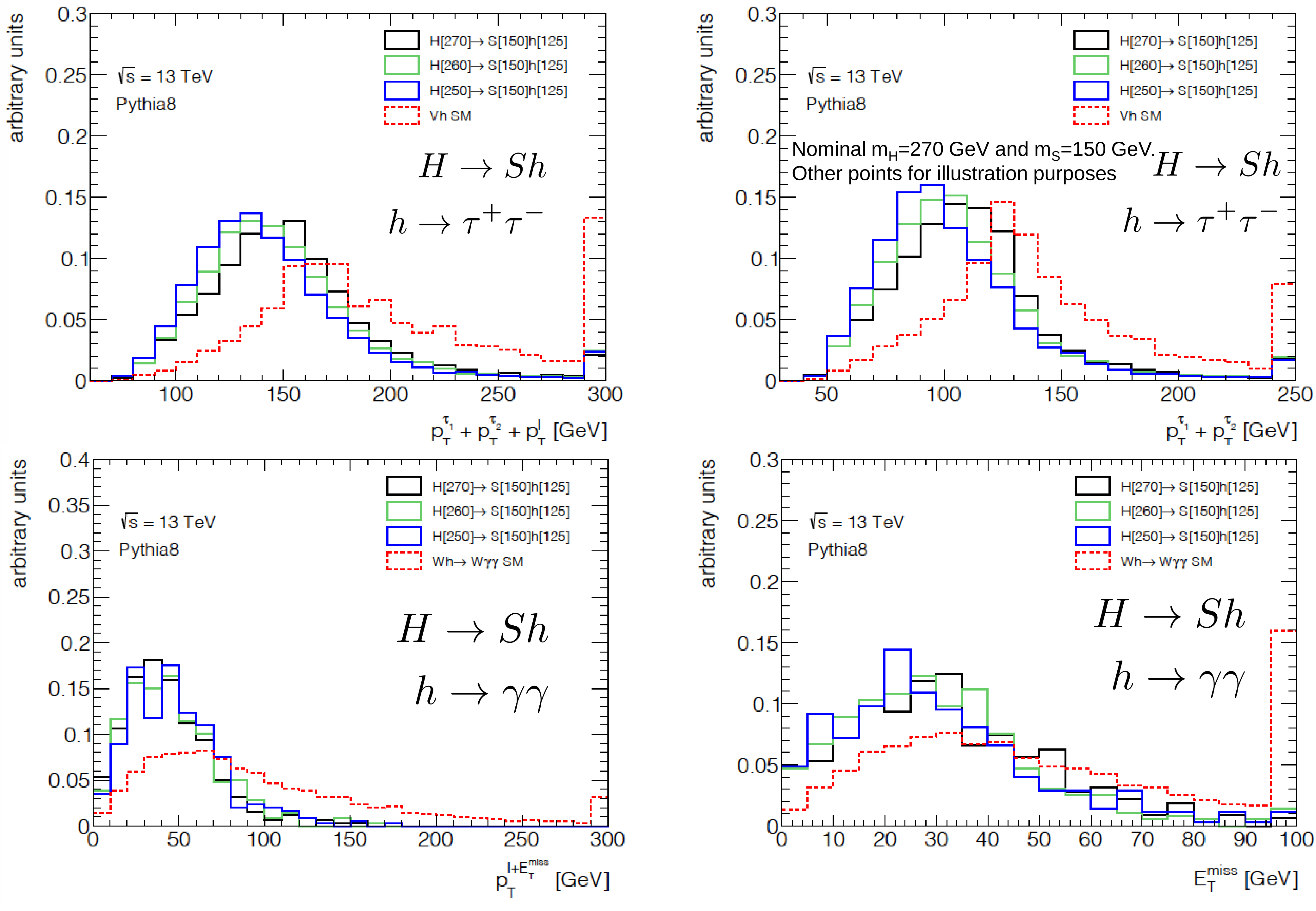
arbitrary units
√s = 13 TeV
Pythia8
H[270]→ S[150]h[125]
H[260]→ S[150]h[125]
H[250]→ S[150]h[125]
Vh SM
$H \to Sh$
$h \to \tau^+\tau^-$
$p_T^{\tau_1} + p_T^{\tau_2} + p_T^{l}$ [GeV]
Nominal m_H=270 GeV and m_S=150 GeV.
Other points for illustration purposes
$p_T^{\tau_1} + p_T^{\tau_2}$ [GeV]
Wh→ Wγγ SM
$h \to \gamma\gamma$
$p_T^{l+E_T^{miss}}$ [GeV]
E_T^{miss} [GeV]

Survey of LHC results on Vh (V=W,Z) production (arXiv:1912.00699)

The BSM (H→Sh) signal appears at low p_{Th} and the SM signal is prevalent at larger P_{Th} (no tuning of parameters)

Include those results from ATLAS and CMS where no requirements on p_{Th} (or correlated observables) is not done or used in an MVA.

Those results where the final state is treated more "inclusively" display elevated signal strengths for Wh production:

$$\mu(Wh) = 2.50 \pm 0.36$$

This represents a 4.2σ deviation from the SM value of 1. BSM signal normalization less than expected from multilepton excesses assuming Br(H→Sh)=100%. Indicates that Br(H→SS) > Br(H→Sh)

Higgs decay	Ref.	Experiment	$\sqrt{s}$, $\mathcal{L}$ TeV, fb^{-1}	Final state	Category	μ	Used in combination	Comments
					DFOS 2j	$2.2^{+2.0}_{-1.9}$	✓	
				2ℓ	SS 1j	$8.4^{+4.3}_{-3.8}$	✓	2ℓ combination: $\mu = 3.7^{+1.9}_{-1.8}$
	[66]	ATLAS	7, 4.5 8, 20.3		SS 2j	$7.6^{+6.0}_{-5.4}$	✓	
				3ℓ	1SFOS	$-2.9^{+2.7}_{-2.1}$	x	$m_{\ell_0\ell_2}$ used as input BDT discriminating variable
WW					0SFOS	$1.7^{+1.9}_{-1.4}$	✓	
	[67]	ATLAS	13, 36.1	3ℓ	1SFOS 0SFOS	$2.3^{+1.2}_{-1.0}$	✓	1SFOS channel uses $m_{\ell_0\ell_2}$ in the BDT but excess driven by 0SFOS
	[68]	CMS	7, 4.9	2ℓ	DFOS 2j	$0.39^{+1.97}_{-1.87}$	✓	Discrepancy at low $m_{\ell\ell}$
			8, 19.4	3ℓ	0+1SFOS	$0.56^{+1.27}_{-0.95}$	✓	
	[69]	CMS	13, 35.9	2ℓ	DFOS 2j	$3.92^{+1.32}_{-1.17}$	✓	Discrepancy at low $m_{\ell\ell}$
				3ℓ	0+1SFOS	$2.23^{+1.76}_{-1.53}$	✓	
	[70]	ATLAS	8, 20.3	1ℓ	$\ell + \tau_h\tau_h$	1.8 ± 3.1	✓	
				2ℓ	$e^{\pm}\mu^{\pm} + \tau_h$	1.3 ± 2.8	✓	
$\tau\tau$	[71]	CMS	7, 4.9	1ℓ	$\ell + \tau_h\tau_h$	-0.33 ± 1.02	x	BDT based on $p_T^{\tau_1} + p_T^{\tau_2}$
			8, 19.7	2ℓ	$e^{\pm}\mu^{\pm} + \tau_h$		x	Split $p_T^{\ell_1} + p_T^{\ell_2} + p_T^{\tau}$ at 130 GeV
	[72]	CMS	13, 35.9	1ℓ 2ℓ	$\ell + \tau_h\tau_h$ $e^{\pm}\mu^{\pm} + \tau_h$	$3.39^{+1.68}_{-1.54}$	✓	
			7, 5.4	$\ell\nu$	One-lepton			
	[73]	ATLAS		$\ell\nu, \nu\nu$	E_T^{miss}	1.0 ± 1.6	x	$E_T^{miss} > 70 - 100$ GeV
			8, 20.3	jj	Hadronic			$p_{Tt}^{\gamma\gamma} > 70$ GeV
			7, 5.1	$\ell\nu$	One-lepton			Split E_T^{miss} at 45 GeV
	[74]	CMS		$\ell\nu, \nu\nu$	E_T^{miss}	$-0.16^{+1.16}_{-0.79}$	x	$E_T^{miss} > 70$ GeV
			8, 19.7	jj	Hadronic			$p_T^{\gamma\gamma} > 13m_{\gamma\gamma}/12$
				$\ell\nu$	One-lepton	$2.41^{+0.71}_{-0.70}$	✓	$p_T^{\ell+E_T^{miss}} < 150$ GeV
						$2.64^{+1.16}_{-0.99}$	x	$p_T^{\ell+E_T^{miss}} > 150$ GeV
$\gamma\gamma$	[75]	ATLAS	13, 139	$\ell\nu, \nu\nu$	E_T^{miss}	-	x	$E_T^{miss} > 75$ GeV
				jj	Hadronic	$0.76^{+0.95}_{-0.83}$	x	$60 < m_{jj} < 120$ GeV
						$3.16^{+1.84}_{-1.72}$	✓	$m_{jj} \in [0, 60] \| [120, 350]$ GeV
				$\ell\nu$	One-lepton	$3.0^{+1.5}_{-1.3}$	x	Superseeded by full Run 2 result
	[76]	CMS	13, 35.6	$\ell\nu, \nu\nu$	E_T^{miss}	-	x	$E_T^{miss} > 85$ GeV
				jj	Hadronic	$5.1^{+2.5}_{-2.3}$	✓	$p_T^{\gamma\gamma}/m_{\gamma\gamma}$ not used
	[77]	CMS	13, 137	$\ell\nu$	One-lepton	$1.31^{+1.42}_{-1.12}$	✓	$p_T^V < 75$ GeV
				jj	Hadronic	$0.89^{+0.89}_{-0.91}$	x	$p_T^{\gamma\gamma}/m_{\gamma\gamma}$ used in BDT
	[78]	ATLAS	13, 139	$\ell\ell\ell + \ell\nu$	Lep-enriched	$1.44^{+1.17}_{-0.93}$	x	Number of jets used in MVA
				$\ell\ell\ell + q\bar{q}$	$2j$			m_{jj} used in MVA
ZZ				$\ell\ell\ell + \ell\nu$	Lep-low p_T^h	$3.21^{+2.49}_{-1.85}$	✓	p_T^h <150 GeV
	[79]	CMS	13, 137.1		Lep-high p_T^h	$0.00^{+1.57}_{-0.00}$	x	p_T^h >150 GeV
				$\ell\ell\ell + q\bar{q}$	$2j$	$0.57^{+1.20}_{-0.57}$	x	$60 < m_{jj} < 120$ GeV

Simplified model predicts low p_{Th}. Due to proximity of the turnover, uncertainties are hard to assess.

Working with collaborators to evaluate robustness of rapidity, where data tends to be more central than prediction

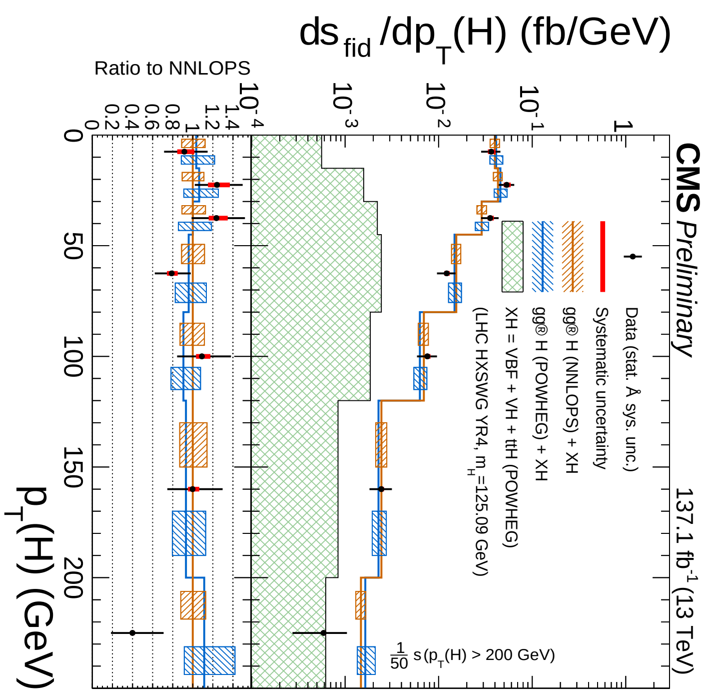

CMS-PAS-HIG-19-001

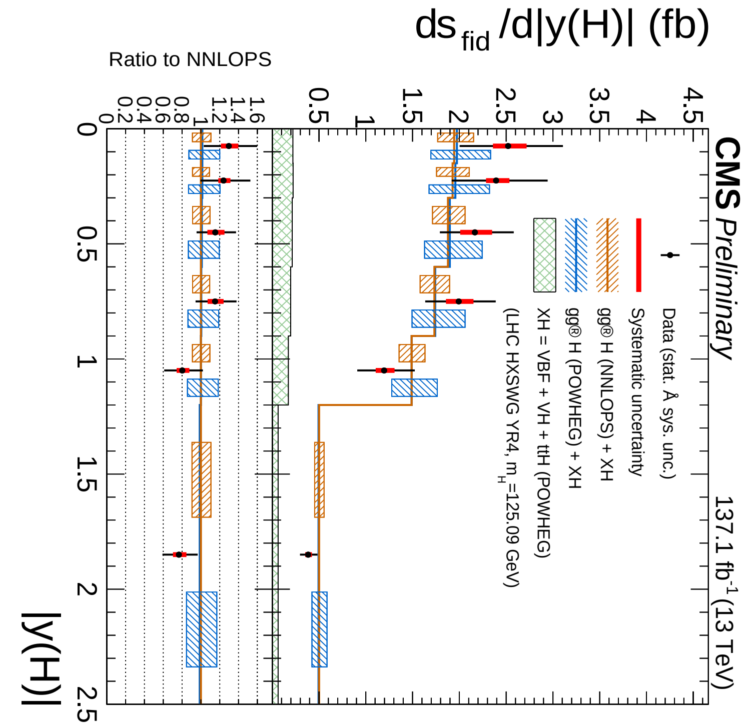

Simplified model predicts more central h production

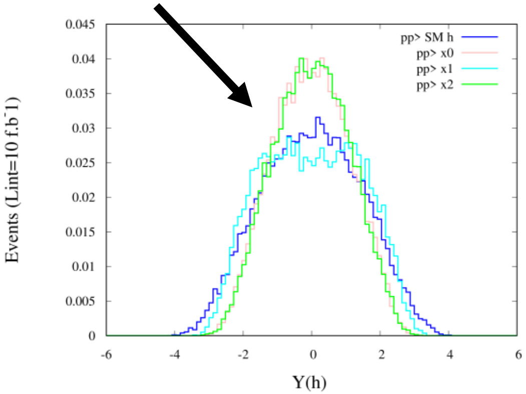

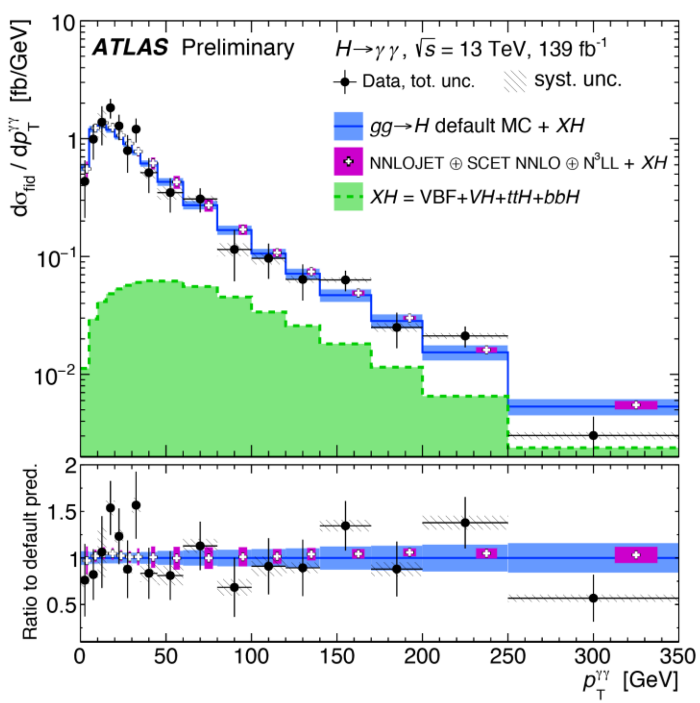

ATLAS-CONF-2019-029

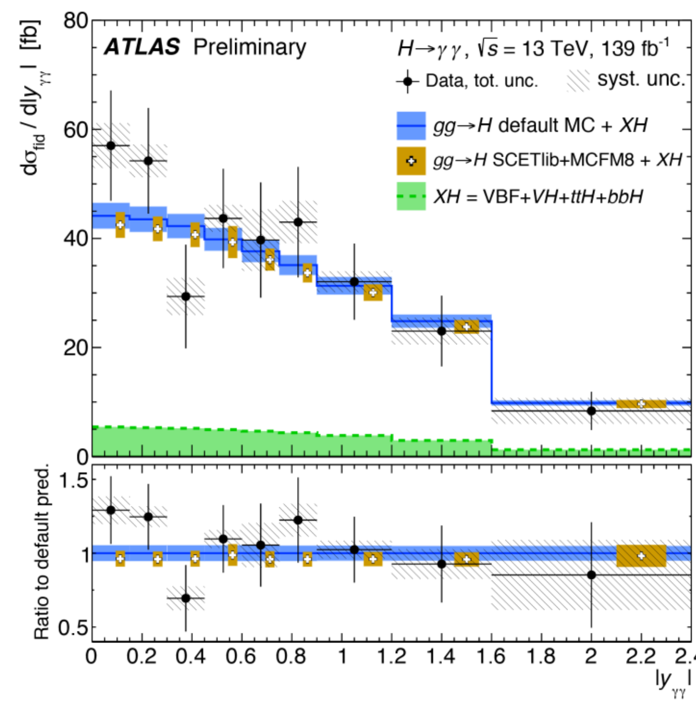

Chin.Phys.C **44 (2020) 6, 063103**

$$\Delta a_\mu = a_\mu^{\mathrm{Exp}} - a_\mu^{\mathrm{SM}} = 2.87(80) \times 10^{-9}$$

The Muon g-2 and the 2HDM+S

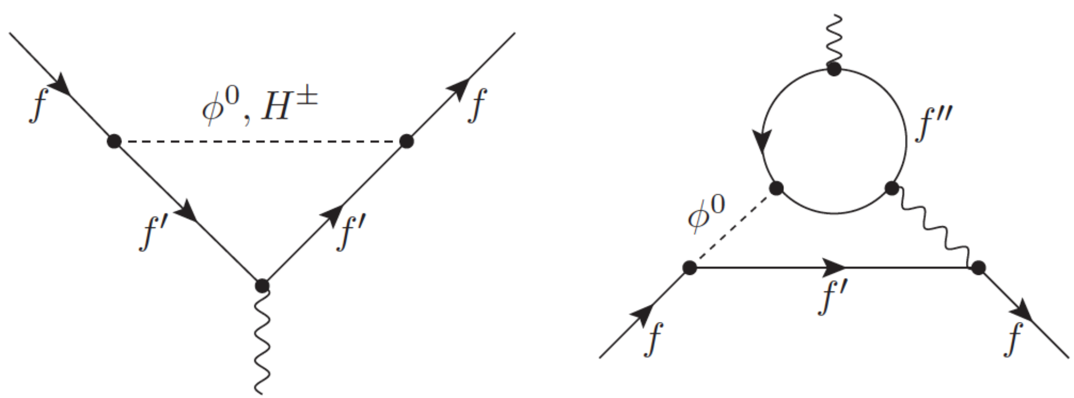

2HDM+S potential with fixed parameters from multi-lepton anomalies at the LHC

$$
\begin{aligned}
&V(\Phi_1, \Phi_2, \Phi_S) \\
&= m_{11}^2 |\Phi_1|^2 + m_{22}^2 |\Phi_2|^2 - m_{12}^2 \left(\Phi_1^\dagger \Phi_2 + \text{h.c.}\right) \\
&+ \frac{\lambda_1}{2}\left(\Phi_1^\dagger \Phi_1\right)^2 + \frac{\lambda_2}{2}\left(\Phi_2^\dagger \Phi_2\right)^2 + \lambda_3 \left(\Phi_1^\dagger \Phi_1\right)\left(\Phi_2^\dagger \Phi_2\right) \\
&+ \lambda_4 \left(\Phi_1^\dagger \Phi_2\right)\left(\Phi_2^\dagger \Phi_1\right) + \frac{\lambda_5}{2}\left[\left(\Phi_1^\dagger \Phi_2\right)^2 + \text{h.c.}\right] \\
&+ \frac{1}{2} m_S^2 \Phi_S^2 + \frac{\lambda_6}{8}\Phi_S^4 + \frac{\lambda_7}{2}\left(\Phi_1^\dagger \Phi_1\right)\Phi_S^2 + \frac{\lambda_8}{2}\left(\Phi_2^\dagger \Phi_2\right)\Phi_S^2
\end{aligned}
$$

Consider extra degrees of freedom in the form of SM singlet vector-like fermions

$$
\mathcal{L} \supset -y_{f'}^S \overline{l_R} \Phi_S f_L' - \sum_{i=1}^{2} y_{f'}^i \overline{L_l} \Phi_i f_R' + \text{h.c.},
$$

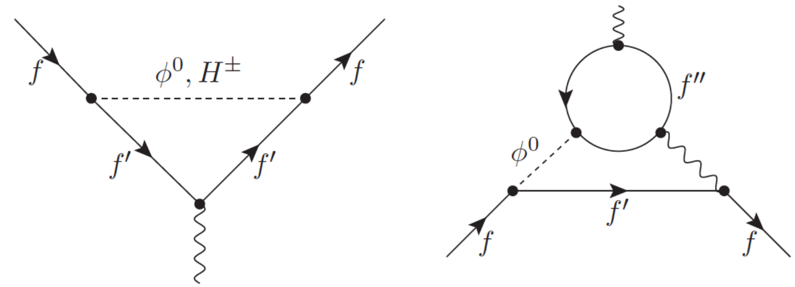

Allowed fermion masses with different choices of Yukawa couplings

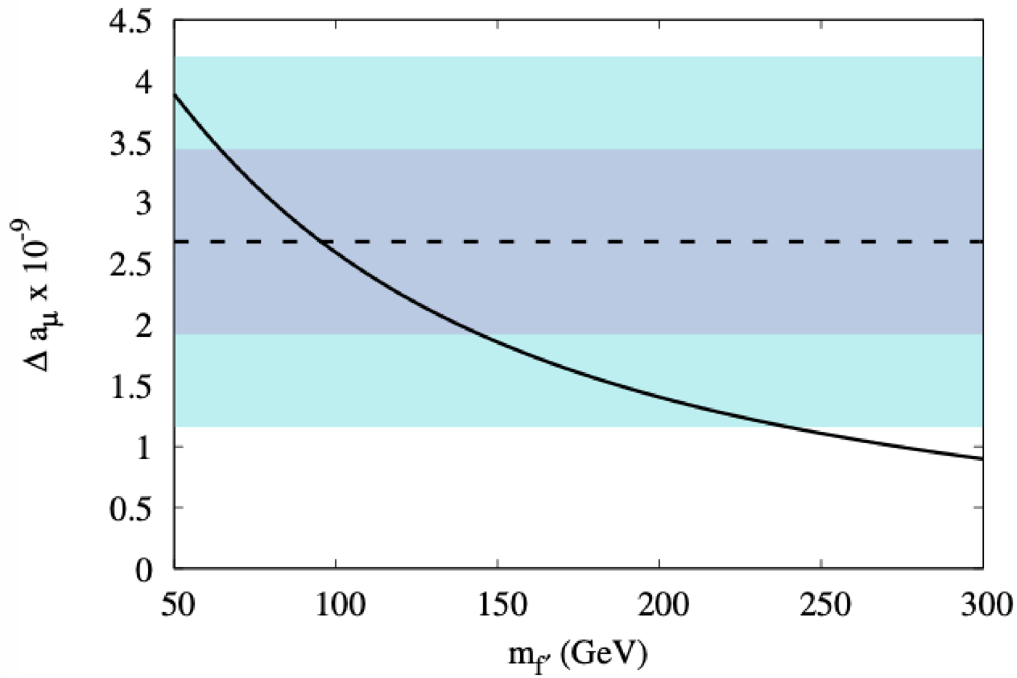

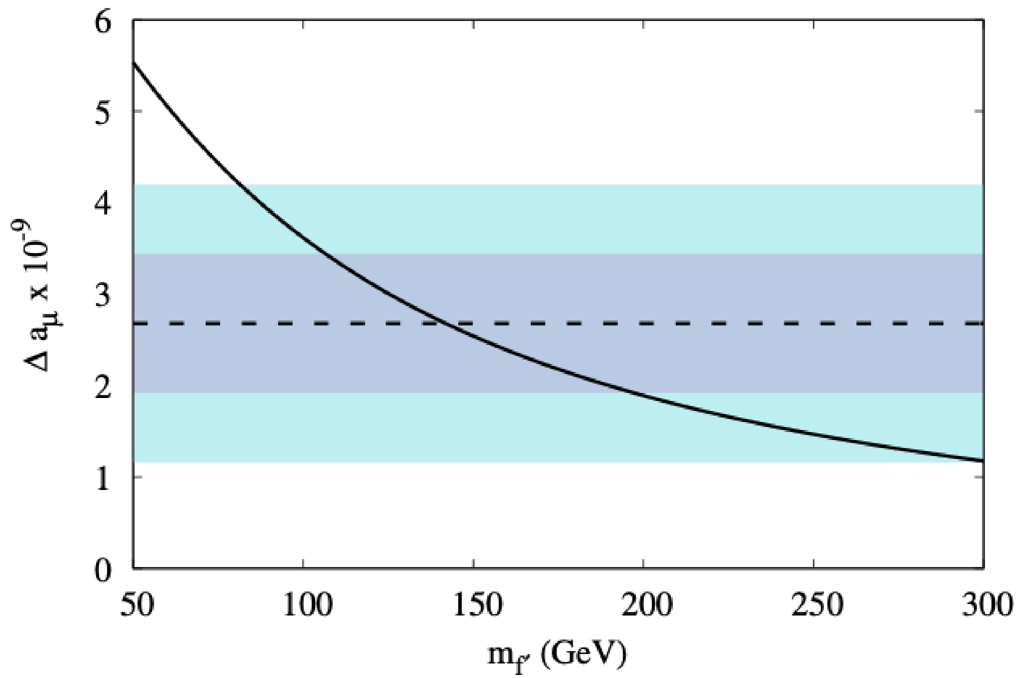

G.Beck, E.Malwa, M.Kumar, R.Temo and B.M. et al. to appear

The multo-lepton anomalies and the SKA

LHC-SKA connection

Effective theory for Weakly Interacting Massive Particles (WIMPs)

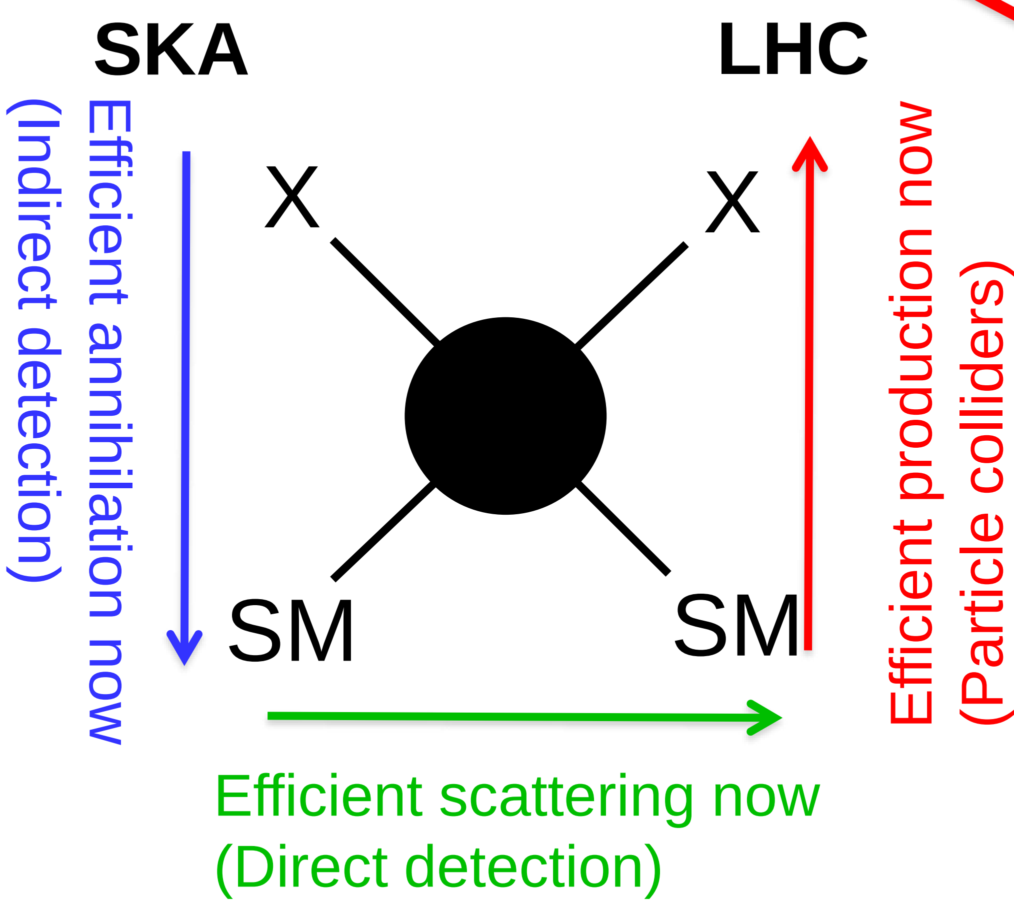

Name	Operator	Coefficient
D1	$\bar{\chi}\chi\bar{q}q$	m_q/M_*^3
D2	$\bar{\chi}\gamma^5\chi\bar{q}q$	im_q/M_*^3
D3	$\bar{\chi}\chi\bar{q}\gamma^5 q$	im_q/M_*^3
D4	$\bar{\chi}\gamma^5\chi\bar{q}\gamma^5 q$	m_q/M_*^3
D5	$\bar{\chi}\gamma^\mu\chi\bar{q}\gamma_\mu q$	$1/M_*^2$
D6	$\bar{\chi}\gamma^\mu\gamma^5\chi\bar{q}\gamma_\mu q$	$1/M_*^2$
D7	$\bar{\chi}\gamma^\mu\chi\bar{q}\gamma_\mu\gamma^5 q$	$1/M_*^2$
D8	$\bar{\chi}\gamma^\mu\gamma^5\chi\bar{q}\gamma_\mu\gamma^5 q$	$1/M_*^2$
D9	$\bar{\chi}\sigma^{\mu\nu}\chi\bar{q}\sigma_{\mu\nu}q$	$1/M_*^2$
D10	$\bar{\chi}\sigma_{\mu\nu}\gamma^5\chi\bar{q}\sigma_{\alpha\beta}q$	i/M_*^2
D11	$\bar{\chi}\chi G_{\mu\nu}G^{\mu\nu}$	$\alpha_s/4M_*^3$
D12	$\bar{\chi}\gamma^5\chi G_{\mu\nu}G^{\mu\nu}$	$i\alpha_s/4M_*^3$
D13	$\bar{\chi}\chi G_{\mu\nu}\tilde{G}^{\mu\nu}$	$i\alpha_s/4M_*^3$
D14	$\bar{\chi}\gamma^5\chi G_{\mu\nu}\tilde{G}^{\mu\nu}$	$\alpha_s/4M_*^3$

Dark matter annihilation.
Leptons, photons and protons
from the decays of S.

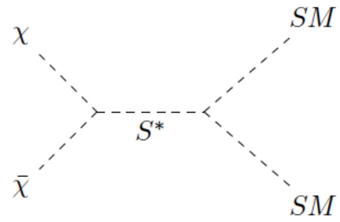

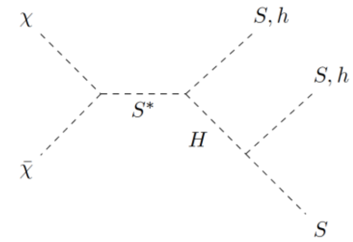

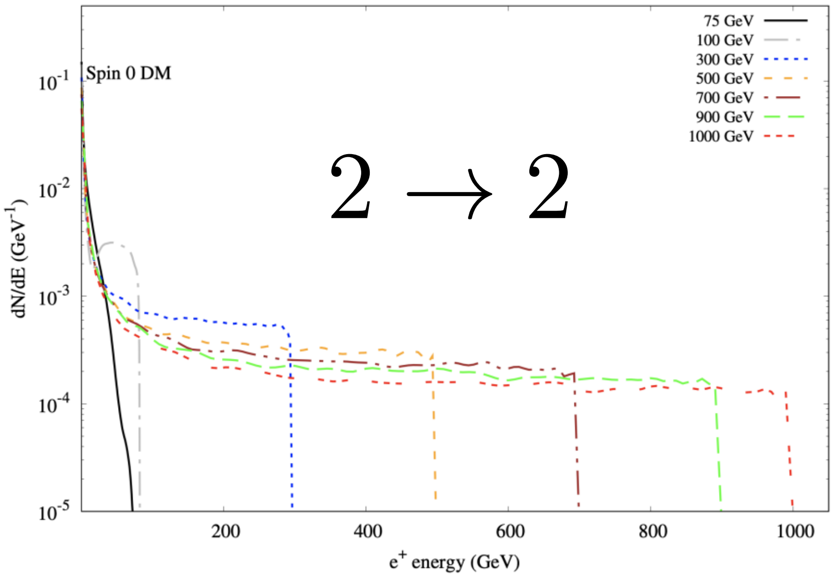

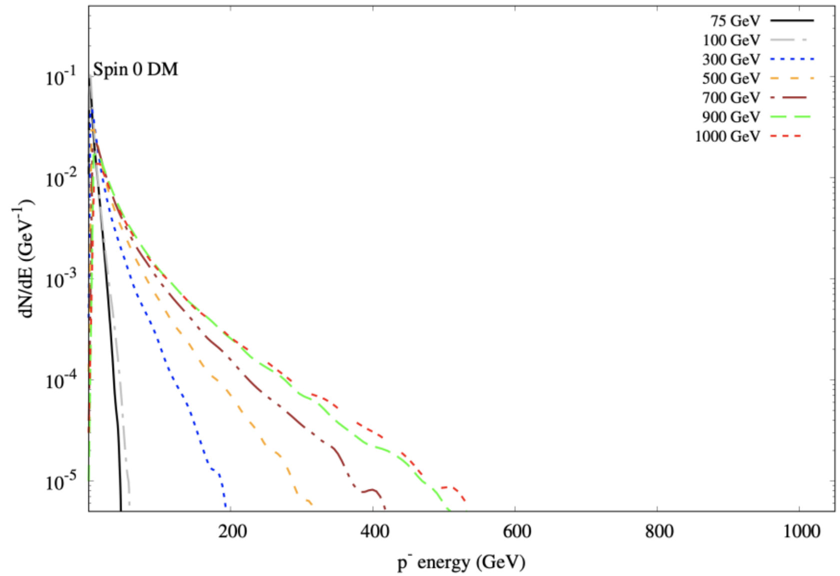

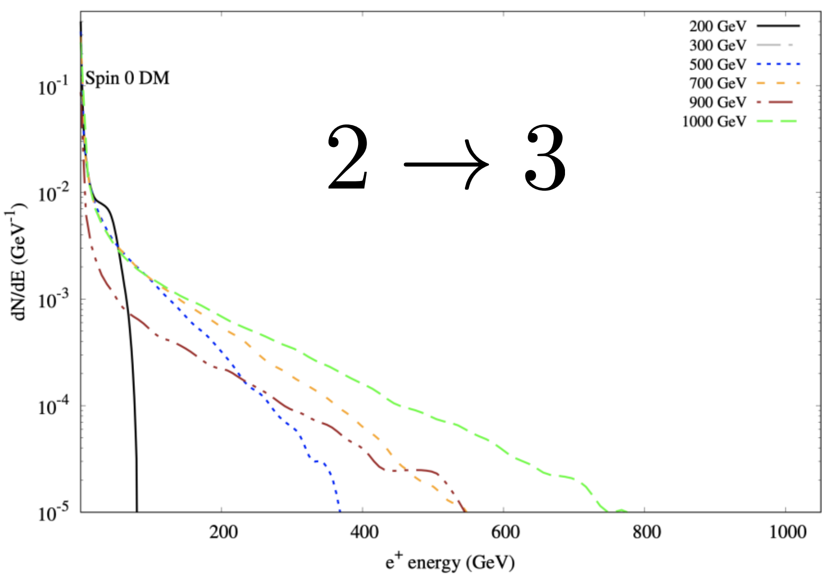

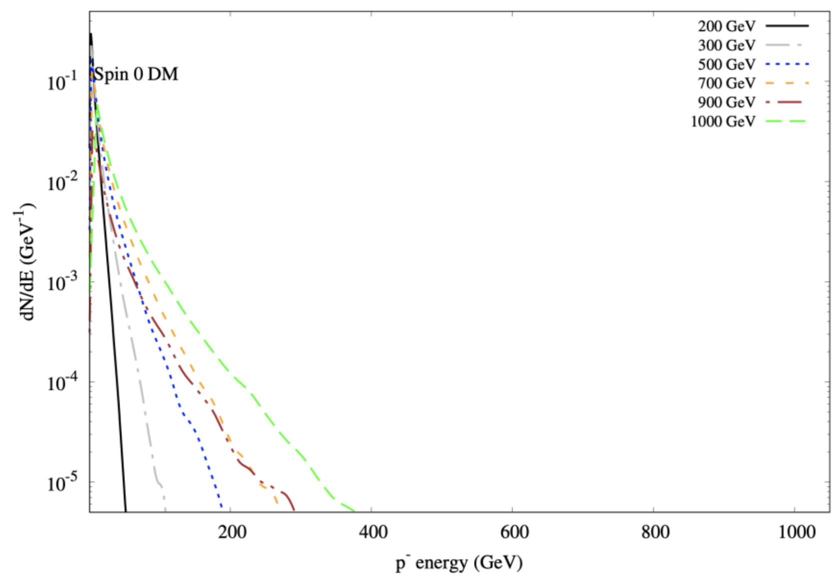

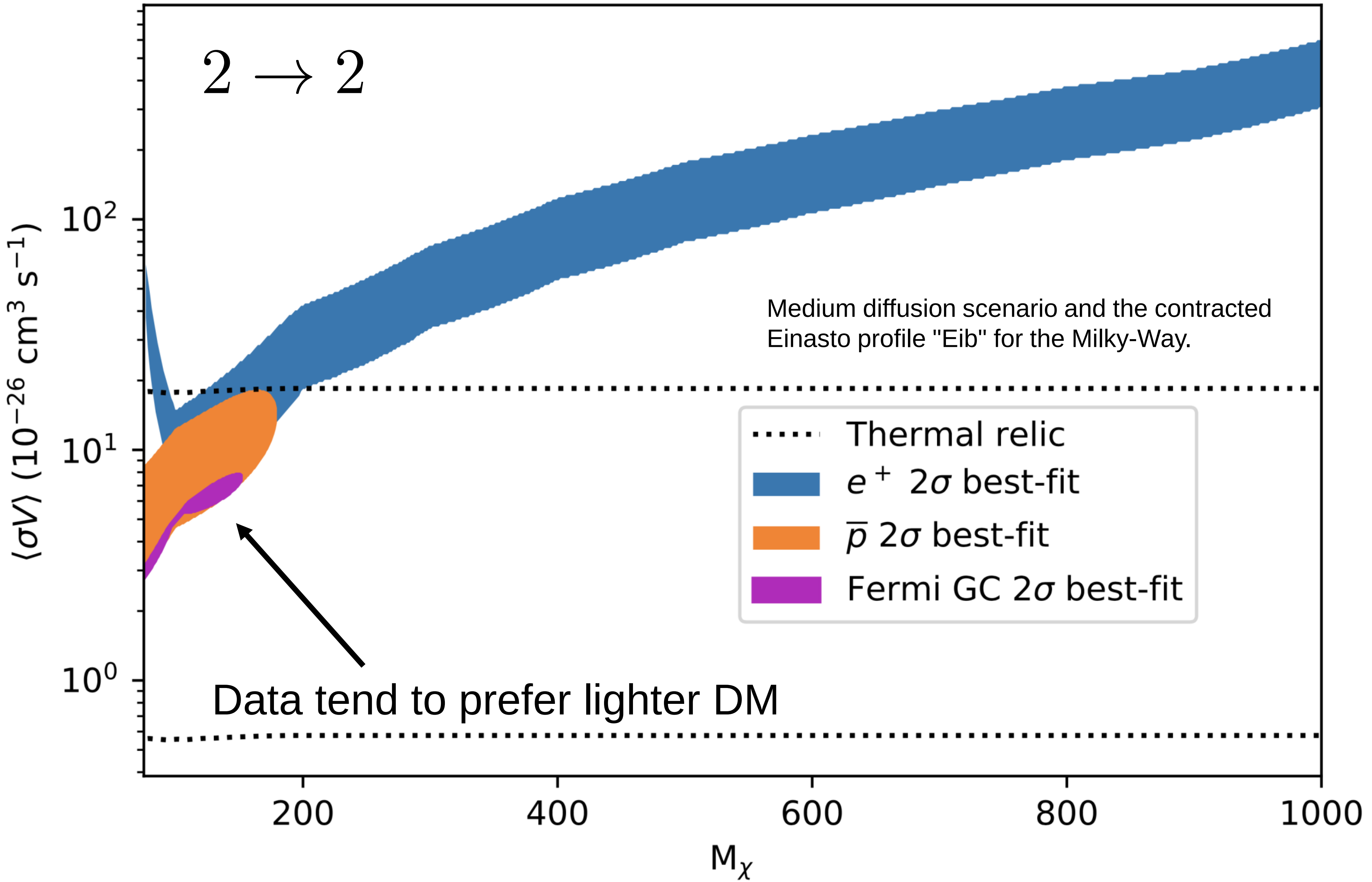

$2 \to 2$
Medium diffusion scenario and the contracted
Einasto profile "Eib" for the Milky-Way.
Thermal relic
e^+ 2σ best-fit
$\bar{p}$ 2σ best-fit
Fermi GC 2σ best-fit
Data tend to prefer lighter DM
$\langle\sigma V\rangle$ (10^{-26} cm^3 s^{-1})
10^2
10^1
10^0
200
400
600
800
1000
M_χ

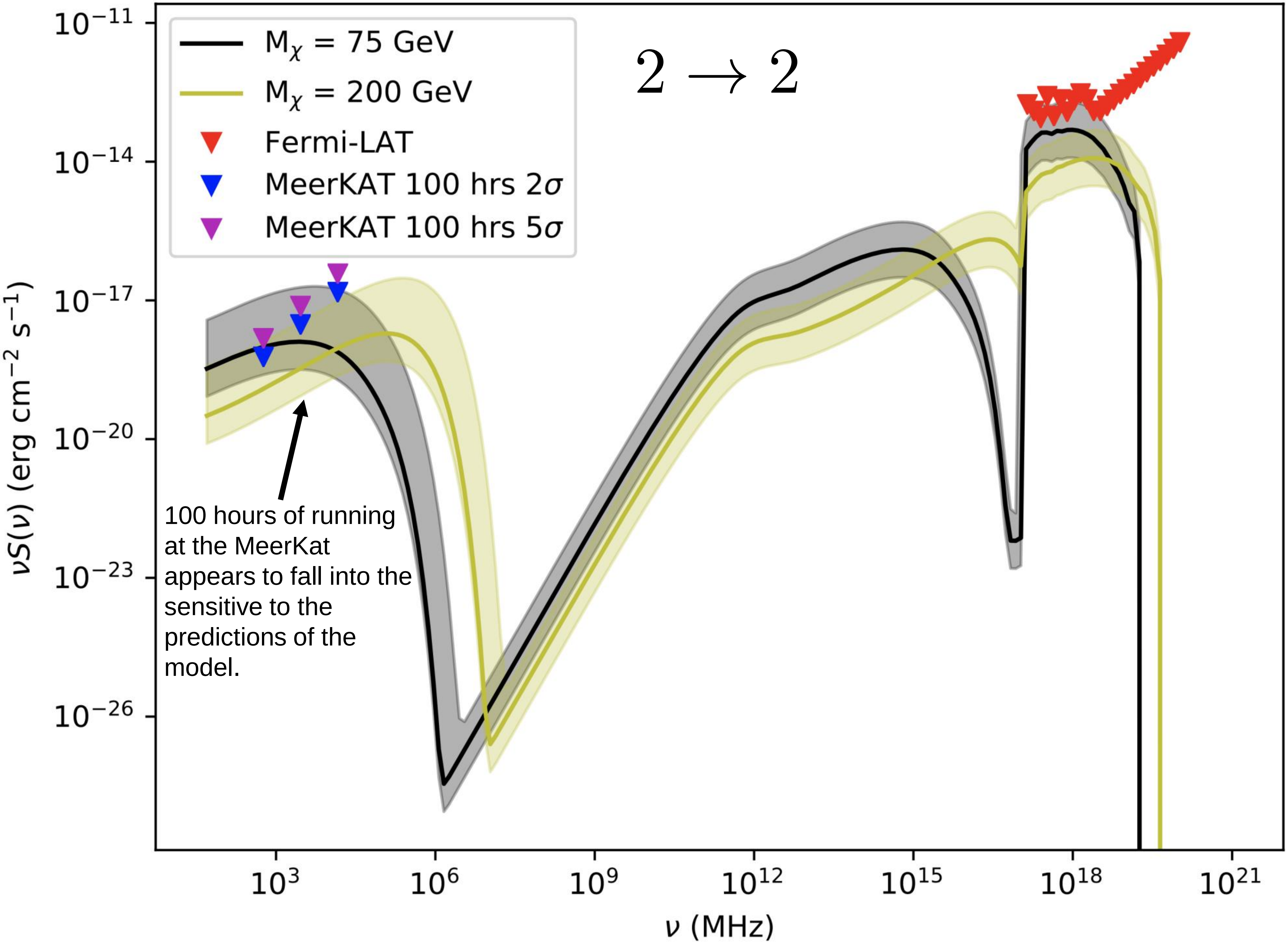

M_χ = 75 GeV
M_χ = 200 GeV
Fermi-LAT
MeerKAT 100 hrs 2σ
MeerKAT 100 hrs 5σ
$2 \rightarrow 2$
100 hours of running at the MeerKat appears to fall into the sensitive to the predictions of the model.
$\nu S(\nu)$ (erg cm^{-2} s^{-1})
ν (MHz)
10^{-11}
10^{-14}
10^{-17}
10^{-20}
10^{-23}
10^{-26}
10^{3}
10^{6}
10^{9}
10^{12}
10^{15}
10^{18}
10^{21}

Outlook and Conclusions

- Discrepancies in multi-lepton final states at LHC w.r.t. current MCs are not statistical fluctuations
  - They appear in corners of the phase-space dominated by different processes: Wt/tt, VV, ttV
    - Hard to explain with MC mismodelling
  - Discrepancies interpreted with simplified model where $H \rightarrow Sh$, S is treated as SM Higgs-like and one parameter is floated
- Features of the Higgs data from LHC agree with predictions the simplified model used here
- Further strengthens the need for precise measurement of Higgs couplings in e^+e^- and pp/ep
- Connection made with excesses in astro-physics, where MeerKat has sensitivity to probe

Additional Slides

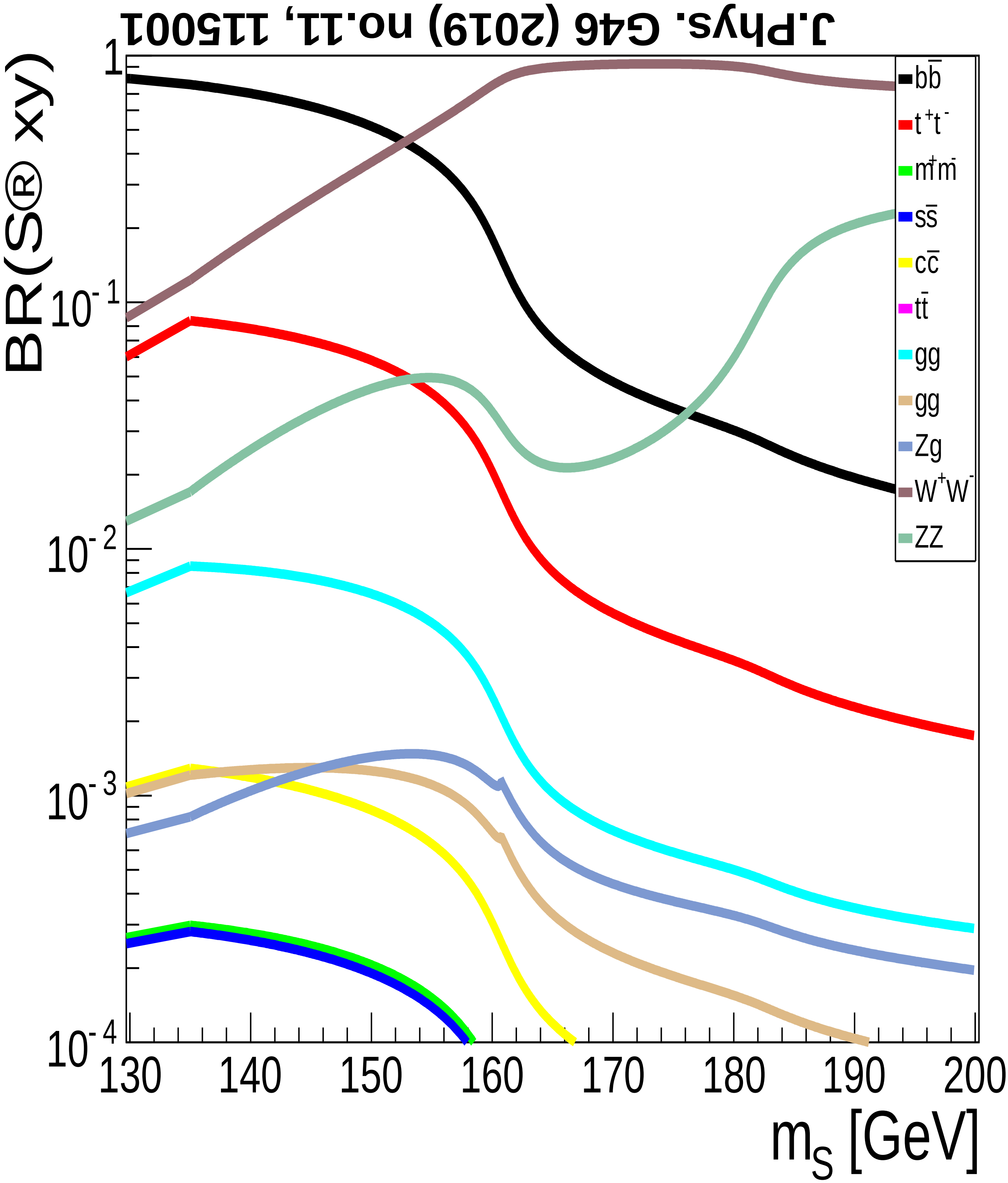

For simplicity we will assume that the S decays like the SM Higgs boson

J.Phys. G46 (2019) no.11, 115001

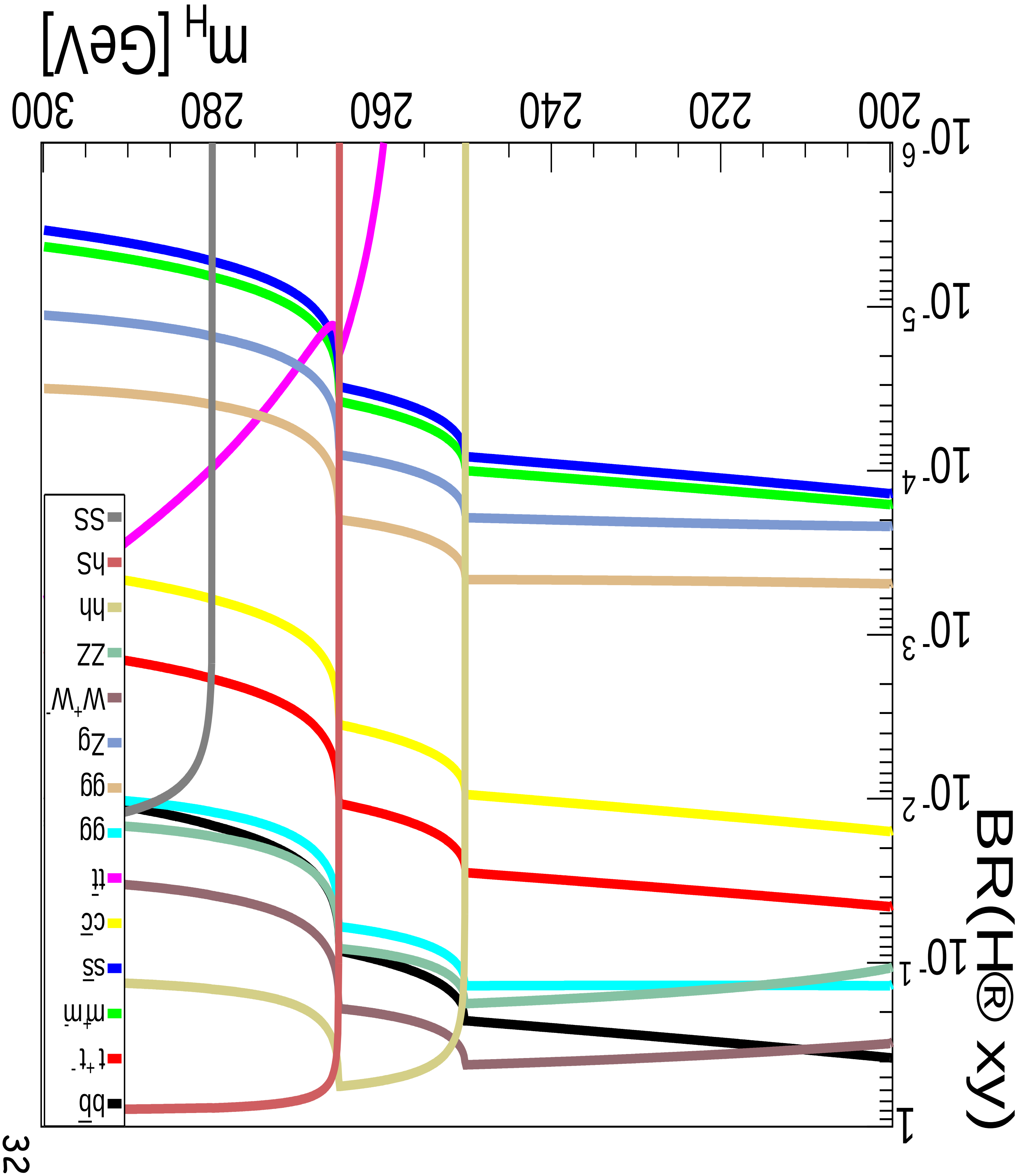

Masses in the 2HDM+S

$$\begin{pmatrix} H_1 \\ H_2 \\ H_3 \end{pmatrix} = \mathbb{R} \begin{pmatrix} \rho_1 \\ \rho_2 \\ \rho_S \end{pmatrix},$$

Mass-matrix for the CP-even scalar sector will modified with respect to 2HDM and that needs a 3 x3 matrix (three mixing angles). Couplings are modified.

$$\mathbb{R} = \begin{pmatrix} c_{\alpha_1} c_{\alpha_2} & s_{\alpha_1} c_{\alpha_2} & s_{\alpha_2} \\ -(c_{\alpha_1} s_{\alpha_2} s_{\alpha_3} + s_{\alpha_1} c_{\alpha_3}) & c_{\alpha_1} c_{\alpha_3} - s_{\alpha_1} s_{\alpha_2} s_{\alpha_3} & c_{\alpha_2} s_{\alpha_3} \\ -c_{\alpha_1} s_{\alpha_2} s_{\alpha_3} + s_{\alpha_1} s_{\alpha_3} & -(c_{\alpha_1} s_{\alpha_3} + s_{\alpha_1} s_{\alpha_2} c_{\alpha_3}) & c_{\alpha_2} c_{\alpha_3} \end{pmatrix}$$

$$M^2_{\mathrm{CP-even}} = \begin{pmatrix} 2\lambda_1 v_1^2 - m_{12} \frac{v_2}{v_1} & m_{12} + \lambda_{345} v_1 v_2 & 2\kappa_1 v_1 v_S \\ m_{12} + \lambda_{345} v_1 v_2 & -m_{12} \frac{v_2}{v_1} + 2\lambda_2 v_2^2 & 2\kappa_2 v_2 v_S \\ 2\kappa_1 v_1 v_S & 2\kappa_2 v_2 v_S & \frac{1}{3} \lambda_S v_S^2 \end{pmatrix}$$

$$
\begin{aligned}
m_{H_1}^2 &= v_S \sin\alpha_2 \left[\lambda_7 v \cos\alpha_1 \cos\alpha_2 \cos\beta + \lambda_8 v \sin\alpha_1 \cos\alpha_2 \sin\beta + \lambda_6 v_S \sin\alpha_2\right], \\
m_{H_2}^2 &= (\cos\alpha_1 \cos\alpha_3 - \sin\alpha_1 \sin\alpha_2 \sin\alpha_3) \Big[\cos\alpha_1 \cos\alpha_2 \left(\lambda_{345} v^2 \sin\beta \cos\beta - m_{12}^2\right) \\
&\quad + \sin\alpha_1 \cos\alpha_2 \left(m_{12}^2 \cot\beta + \lambda_2 v^2 \sin^2\beta\right) + \lambda_8 v v_S \sin\alpha_2 \sin\beta\Big], \\
m_{H_3}^2 &= (\sin\alpha_1 \sin\alpha_3 - \sin\alpha_2 \cos\alpha_1 \cos\alpha_3) \Big[\cos\alpha_1 \cos\alpha_2 \left(m_{12}^2 \tan\beta + \lambda_1 v^2 \cos^2\beta\right) \\
&\quad + \sin\alpha_1 \cos\alpha_2 \left(\lambda_{345} v^2 \sin\beta \cos\beta - m_{12}^2\right) + \lambda_7 v v_S \sin\alpha_2 \cos\beta\Big]. \qquad (2.17)
\end{aligned}
$$

Perform scans after fixing masses of physical bosons(m_{h1}=125 GeV, m_{h2}=140, m_{h3}=270 GeV, m_A=600 GeV, $m_{H^\pm}$=600 GeV) in addition to the constraints described in arXiv:1711.07874, including the signal Yukawa coupling strength of $\beta_g^2=1.38\pm0.22$ (translated into $\tan^2\beta$)

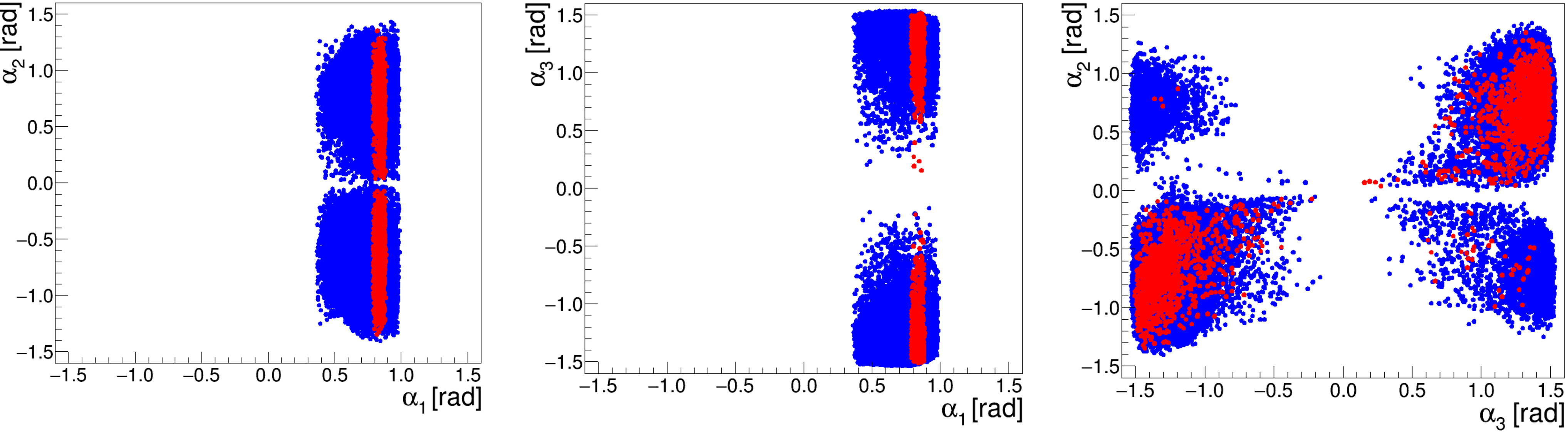

Correlation plots for the three mixing angles and tanβ. Blue (red) points correspond to Br(h→SM) within 10% (20%) of the SM h values (J.Phys. G46 (2019) no.11, 115001)

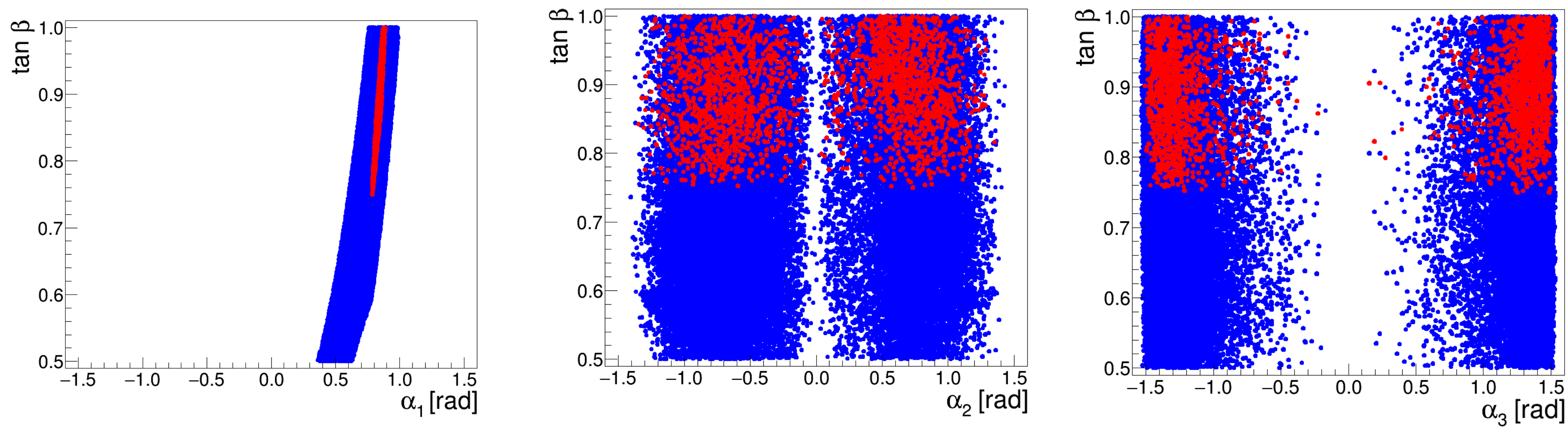

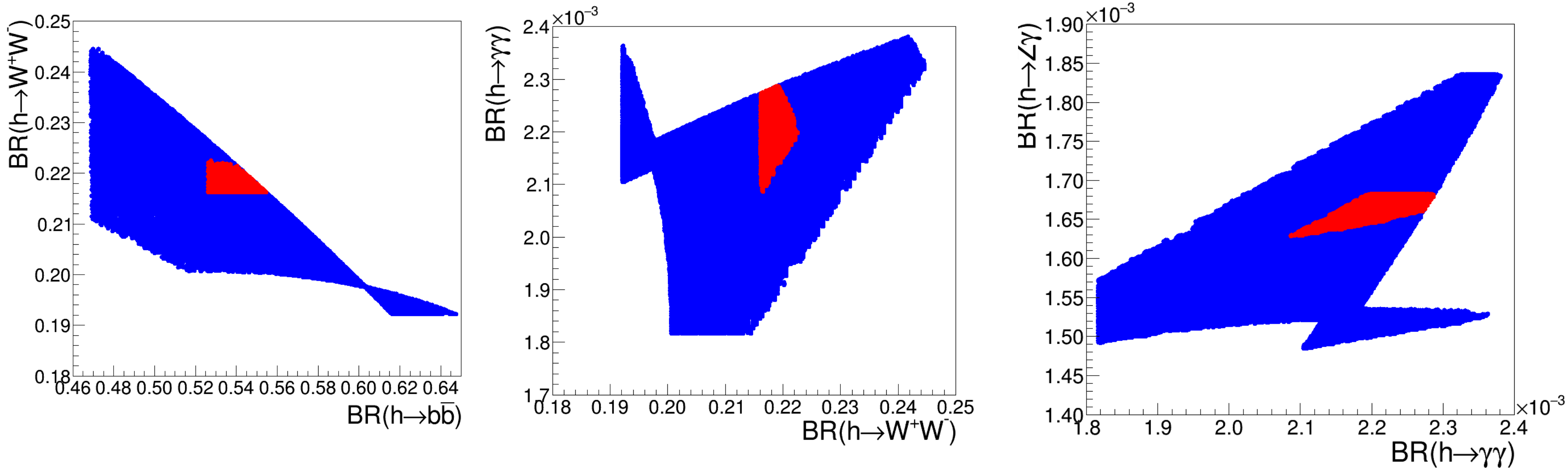

Results using N2HDECAY (arXiv:1612.01309) for one benchmark point

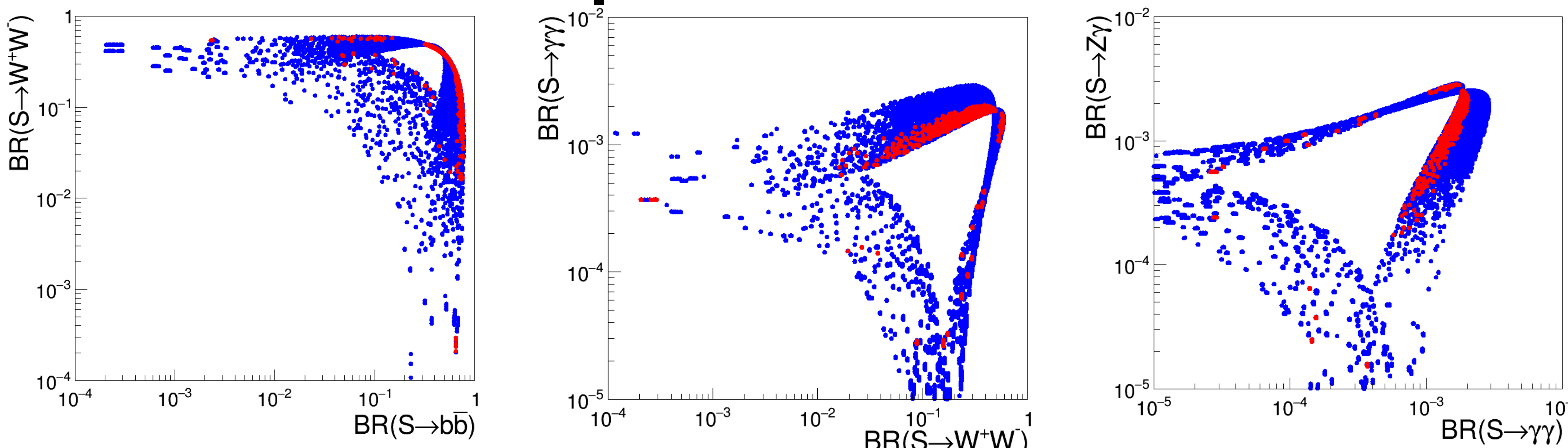

Impact of NNLO QCD in WW

The NNLO QCD corrections shift the m_{ll} spectrum towards larger values.

The discrepancy becomes larger in the region of interest with m_{ll}<100 GeV

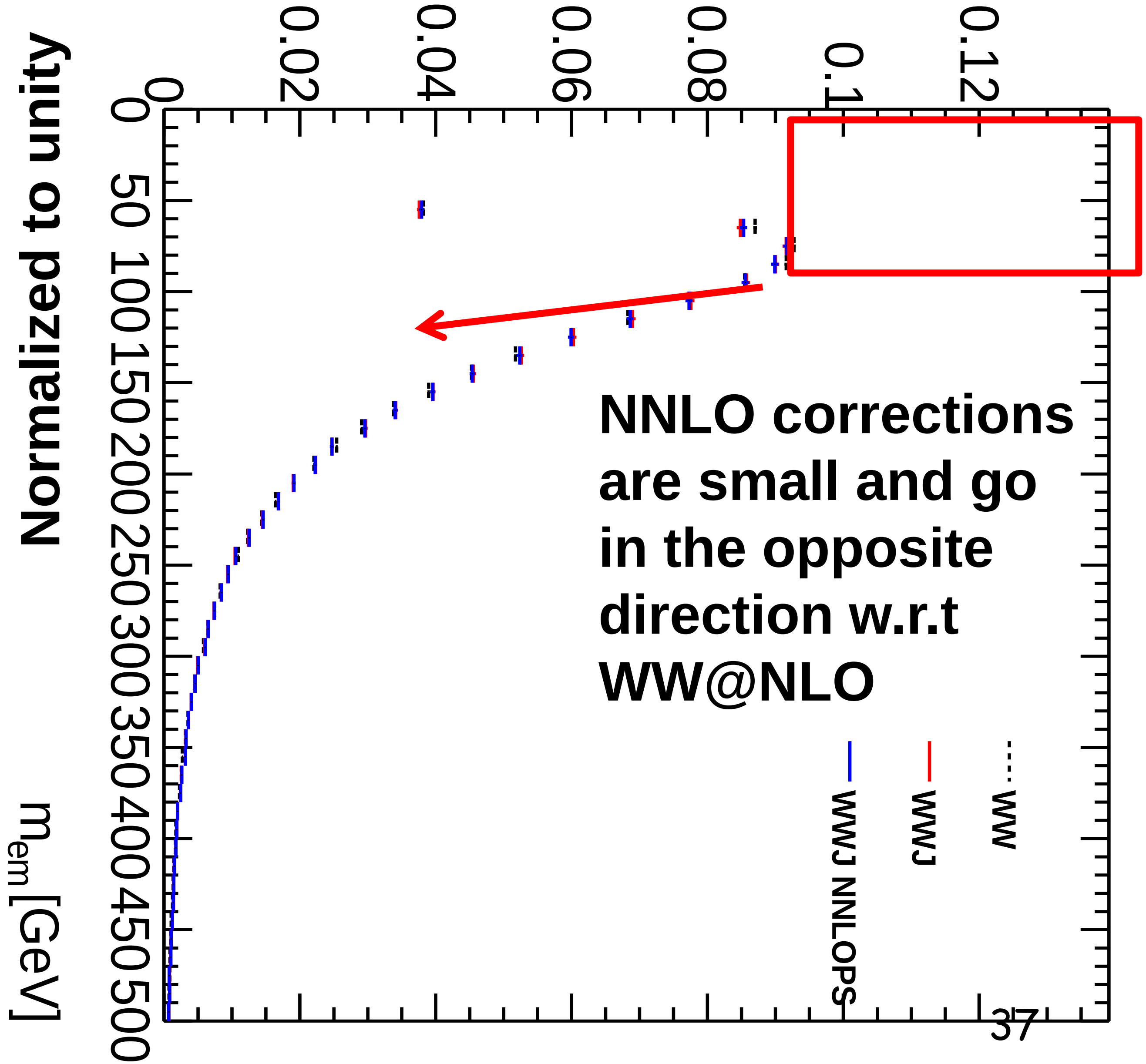

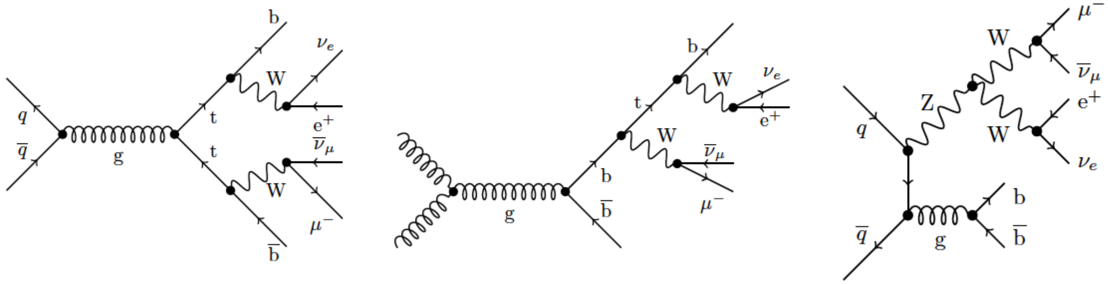

A.Denner, M.Pellen, arXiv:1607.05571

EW corrections are important at high p_T due to Sudakov logarithms. Effect is less than 1% for m_{ll}<100 GeV, where discrepancies are seen.

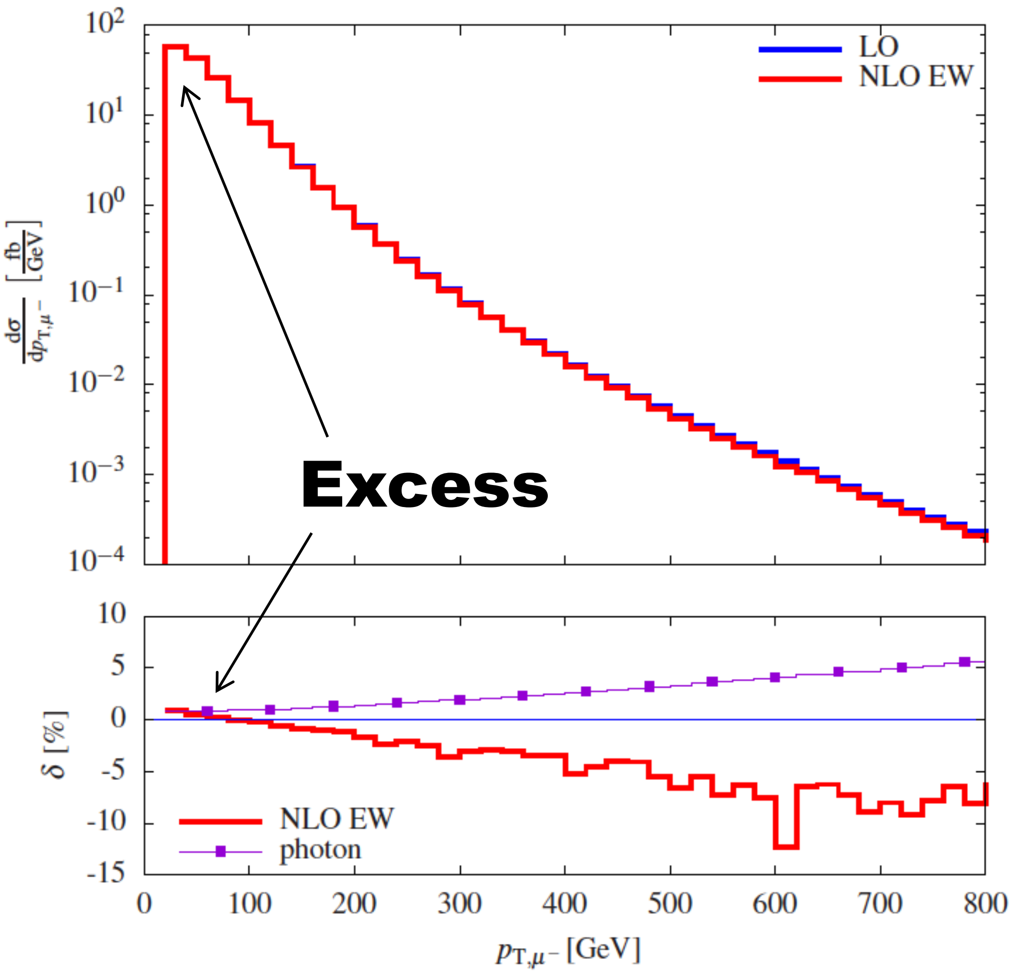

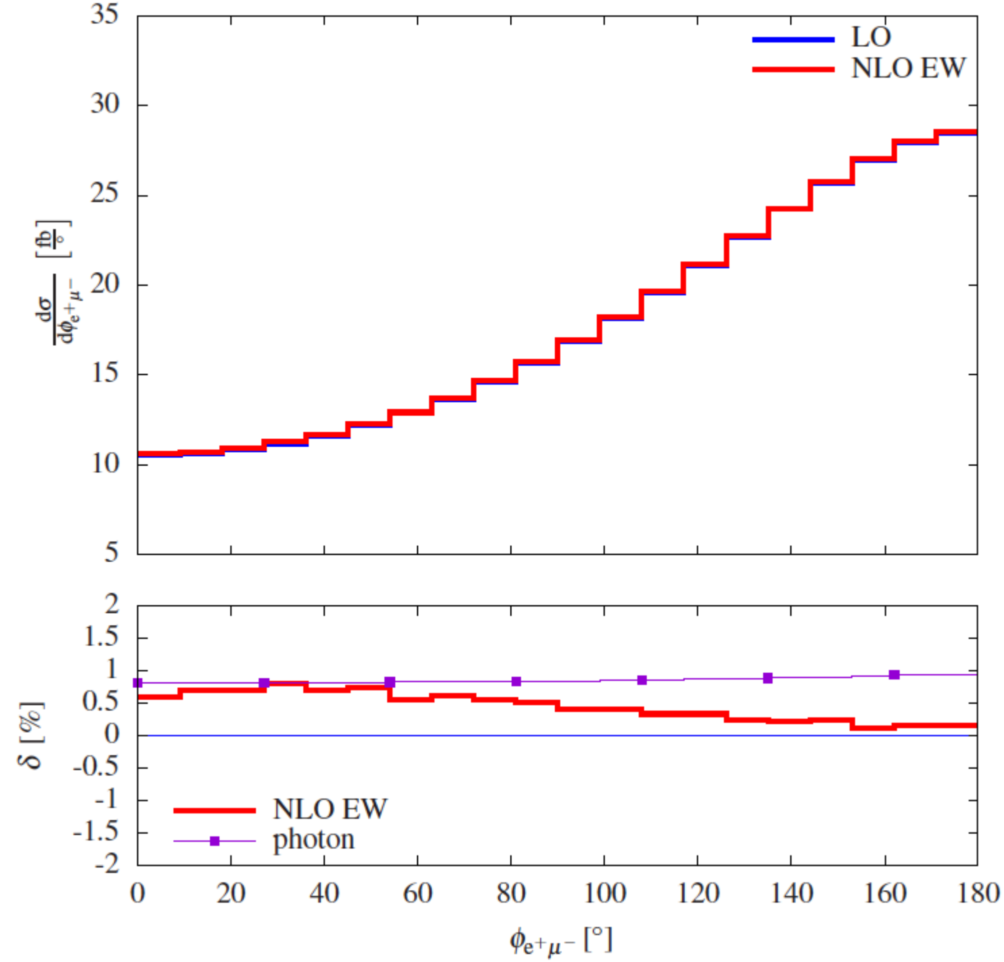

The HistFactory method

K. Cranmer, G. Lewis, L. Moneta, A. Shibata, and W. Verkerke, *HistFactory: A tool for creating statistical models for use with RooFit and RooStats*, CERN-OPEN-2012-016.

- **Constructs a likelihood function from template histograms**
- **Allows for a simple implementation of systematic uncertainties that affect normalisation and/or shape**

$$\mathcal{P}(n_{cb}, a_p \,|\, \phi_p, \alpha_p, \gamma_b) = \prod_{c \in \text{channels}} \prod_{b \in \text{bins}} \text{Pois}(n_{cb}|\nu_{cb}) \cdot G(L_0|\lambda, \Delta_L) \cdot \prod_{p \in \mathbb{S}+\Gamma} f_p(a_p|\alpha_p)$$

In our case, each "channel" is a different measurement.

The Poisson probability for the "expected" and "observed" number of events per bin.

Functional form of luminosity and its variations (not necessary for us).

Functional form of systematic variation with nuisance parameter αp.

3l with Z→ll (ZW cross-section)

CMS PAS SMP-18-002

Errors in the plot are dominated by the 15% uncertainty on normalization to account NLO/NNLO differences. The uncertainty of the shape is much smaller of order of few %

Source	Combined	eee	$ee\mu$	$\mu\mu e$	$\mu\mu\mu$
Electron efficiency	1.9	5.9	3.9	1.9	0
Electron scale	0.3	0.9	0.2	0.6	0
Muon efficiency	1.9	0	0.8	1.8	2.6
Muon scale	0.5	0	0.7	0.3	0.9
Trigger efficiency	1.9	2.0	1.9	1.9	1.8
Jet energy scale	0.9	1.6	1.0	1.7	0.8
B-tagging (id.)	2.6	2.7	2.6	2.6	2.4
B-tagging (mis-id.)	0.9	1.0	0.9	1.0	0.7
Pileup	0.8	0.9	0.3	1.3	1.4
ZZ	0.6	0.7	0.4	0.8	0.5
Nonprompt norm.	1.2	2.0	1.2	1.5	1.0
Nonprompt (EWK subs.)	1.0	1.5	1.0	1.3	0.8
VVV norm.	0.5	0.6	0.6	0.6	0.5
VH norm.	0.2	0.2	0.3	0.2	0.2
$t\bar{t}$ V norm.	0.5	0.5	0.5	0.5	0.5
tZq norm.	0.1	0.1	0.1	0.1	0.1
X+γ norm.	0.3	0.8	0	0.7	0
Total systematic	4.7	7.8	5.8	5.7	4.6
Luminosity	2.8	2.9	2.8	2.9	2.8
Statistical	2.1	6.0	4.8	4.1	3.1
Total experimental	6.0	10.8	8.0	7.5	6.3
Theoretical	0.9	0.9	0.9	0.9	0.9

Systematics that will directly affect the shape (ZZ through X+γ norm.)

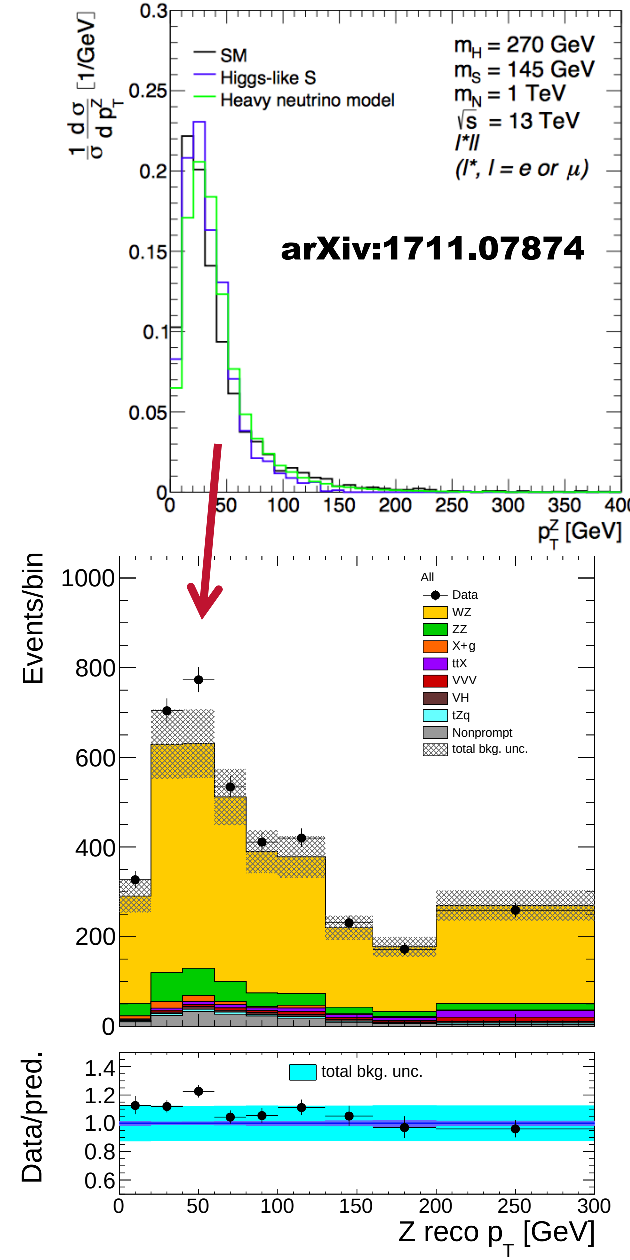

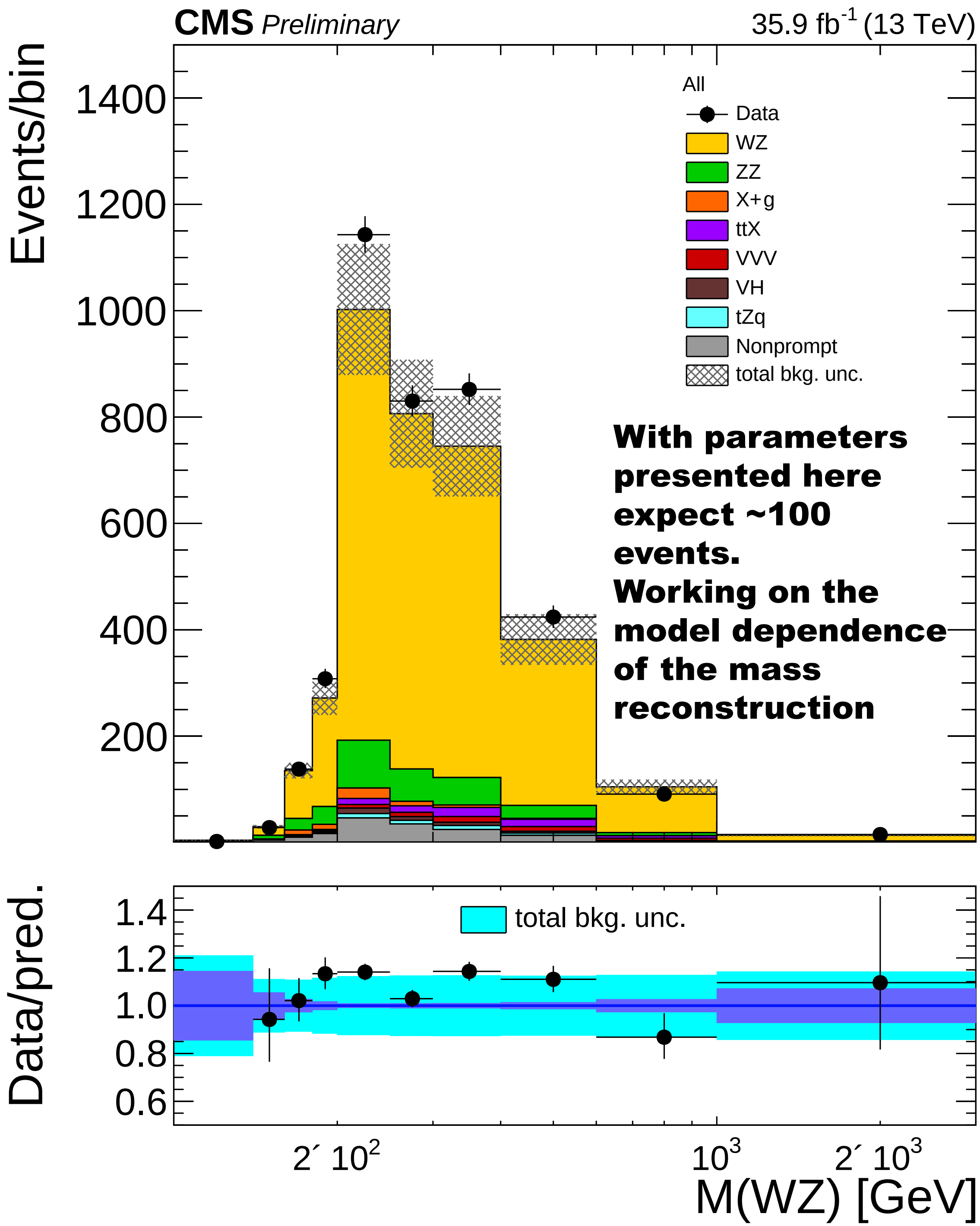

With parameters presented here expect ~100 events.
Working on the model dependence of the mass reconstruction

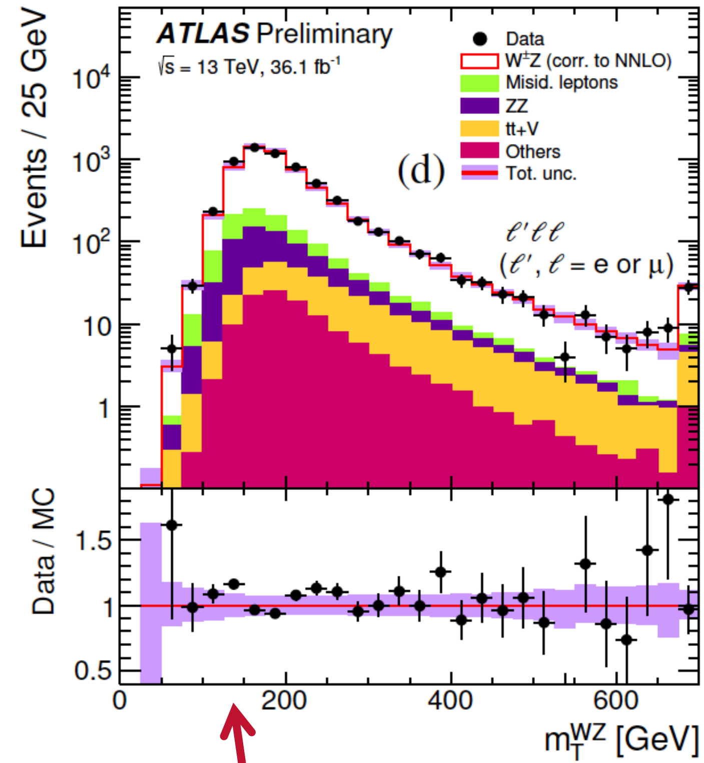

arXiv:1711.07874

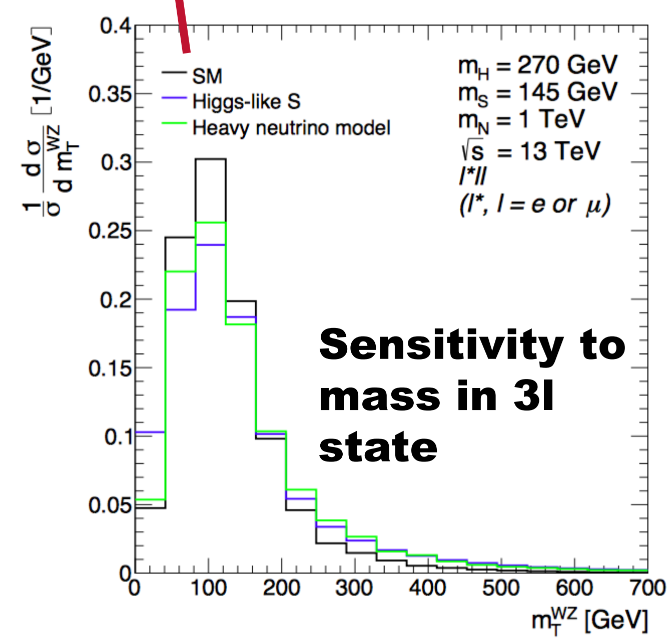

Sensitivity to mass in 3l state

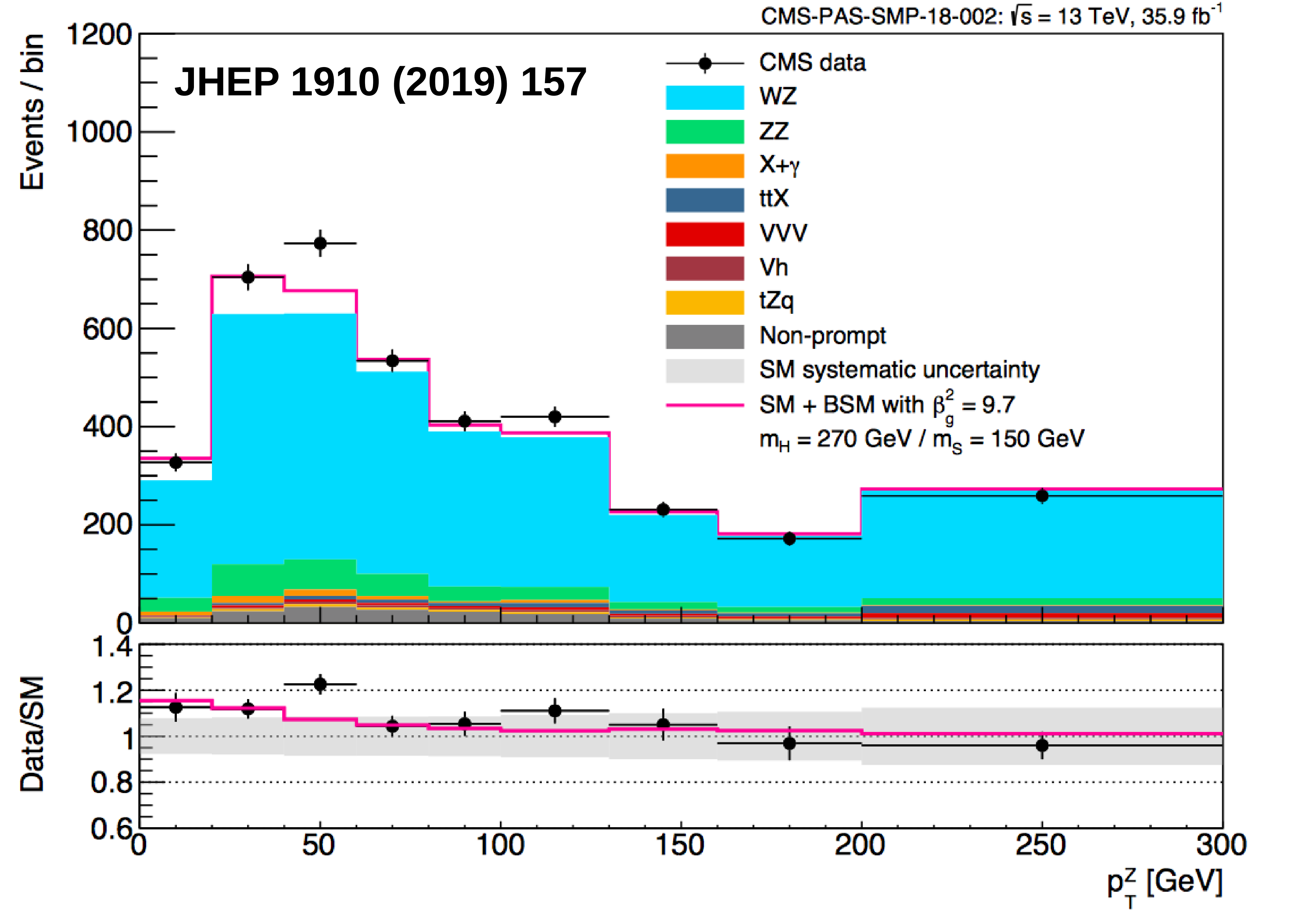
CMS-PAS-SMP-18-002: $\sqrt{s}$ = 13 TeV, 35.9 fb^{-1}
JHEP 1910 (2019) 157
CMS data
WZ
ZZ
X+γ
ttX
VVV
Vh
tZq
Non-prompt
SM systematic uncertainty
SM + BSM with β_g^2 = 9.7
m_H = 270 GeV / m_S = 150 GeV
Events / bin
Data/SM
p_T^Z [GeV]
0
50
100
150
200
250
300
1200
1000
800
600
400
200
1.4
1.2
1
0.8
0.6

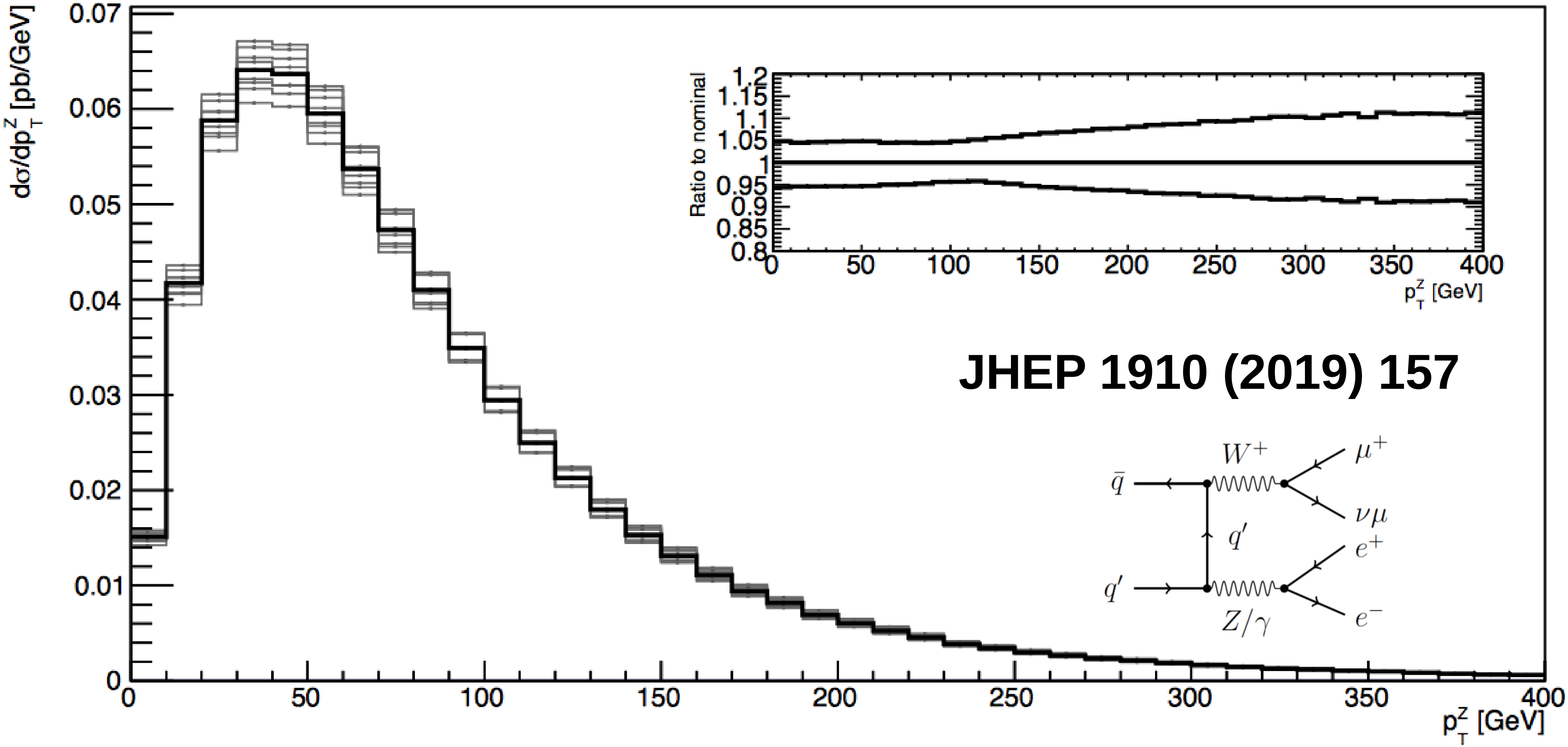

Figure 10: The effects of scale variations in the differential cross section of the SM WZ process as a function of the Z p_{T}. Here, `aMC@NLO` and `Pythia 8` were used to generate the events. The thick black line represents the spectrum at the nominal scale, and each grey line is a variation of the scale. The insert shows the maximum and minimum relative deviations for all scale variations.

The fitting procedure

- **The RooStats workspace is made by HistFactory**
- **From the workspace, a profile likelihood ratio is calculated,**

$$\lambda\left(\beta_g^2\right) = \frac{L\left(\beta_g^2 \mid \hat{\hat{\theta}}\right)}{L\left(\hat{\beta}_g^2 \mid \hat{\theta}\right)}$$

(here θ denotes the nuisance parameters)

- **The best-fit value of β_g^2 is then calculated as the minimum of -2log(λ), with an error corresponding to a unit of deviation in this quantity from the best-fit point**
- **The significance is calculated as √(-2 log λ(0)), since β_g^2 = 0 corresponds to the SM-only hypothesis**

Excesses in di-leptons with full-jet veto not included above

Run 1, J.Phys. G45 (2018) no.11, 115003

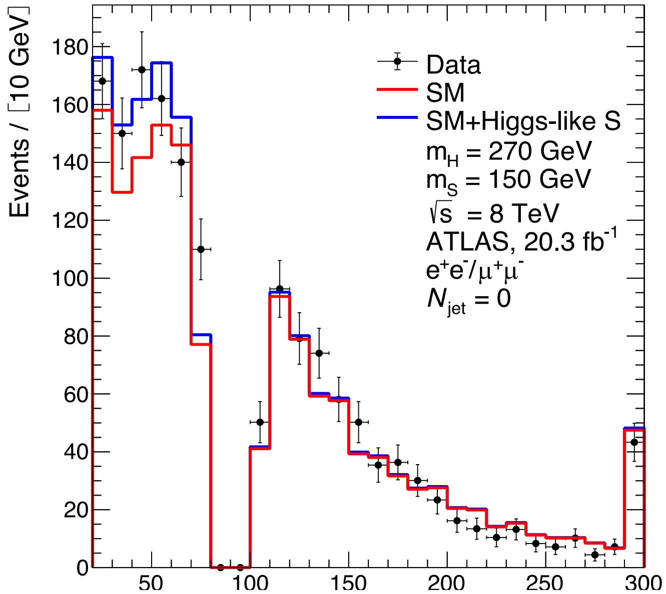

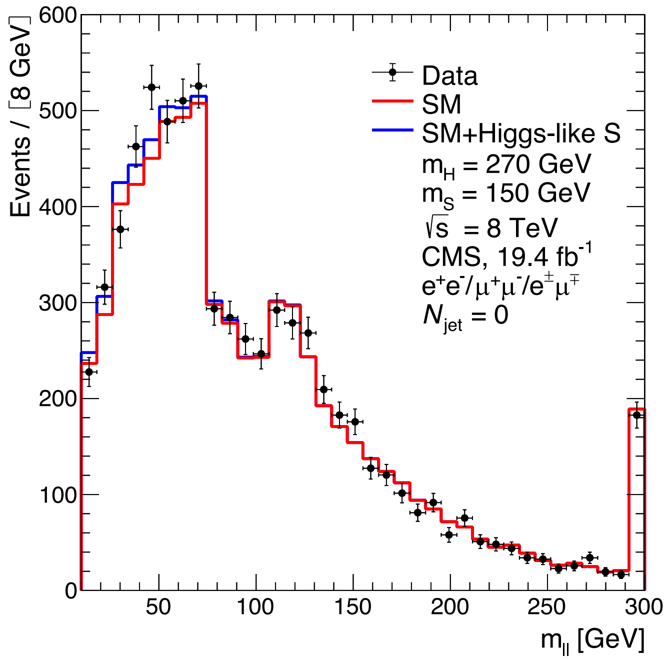

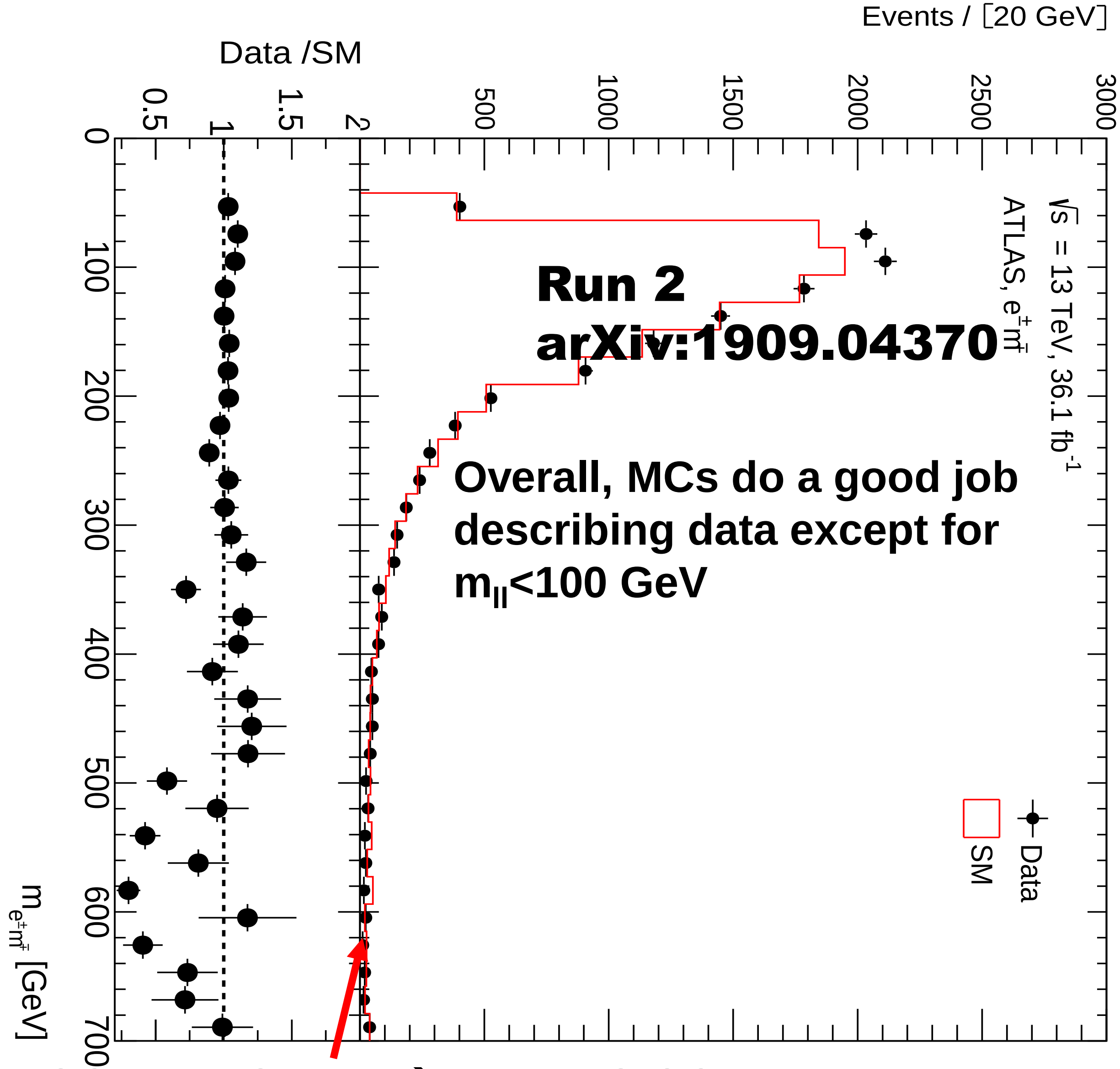

Run 2
arXiv:1909.04370

Overall, MCs do a good job describing data except for m_{ll}<100 GeV

QCD NNLO to qq→WW, NLO QCD to gg→WW and NLO EW corrections applied

Results not included in the combination

arXiv:1910.08819

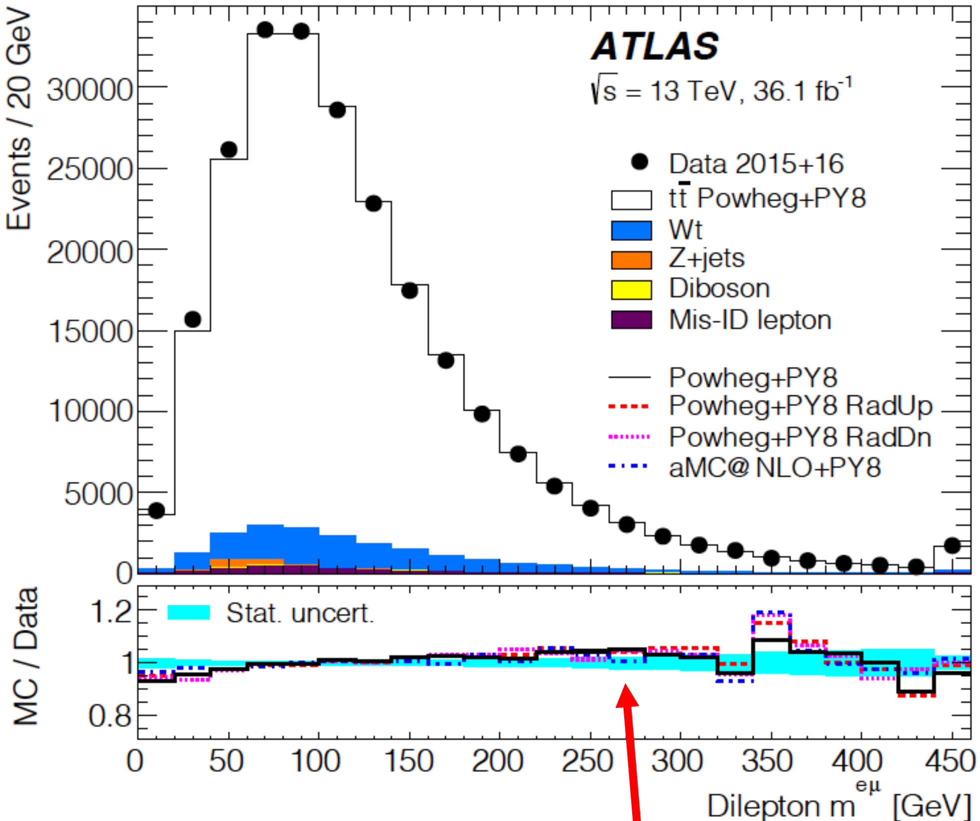

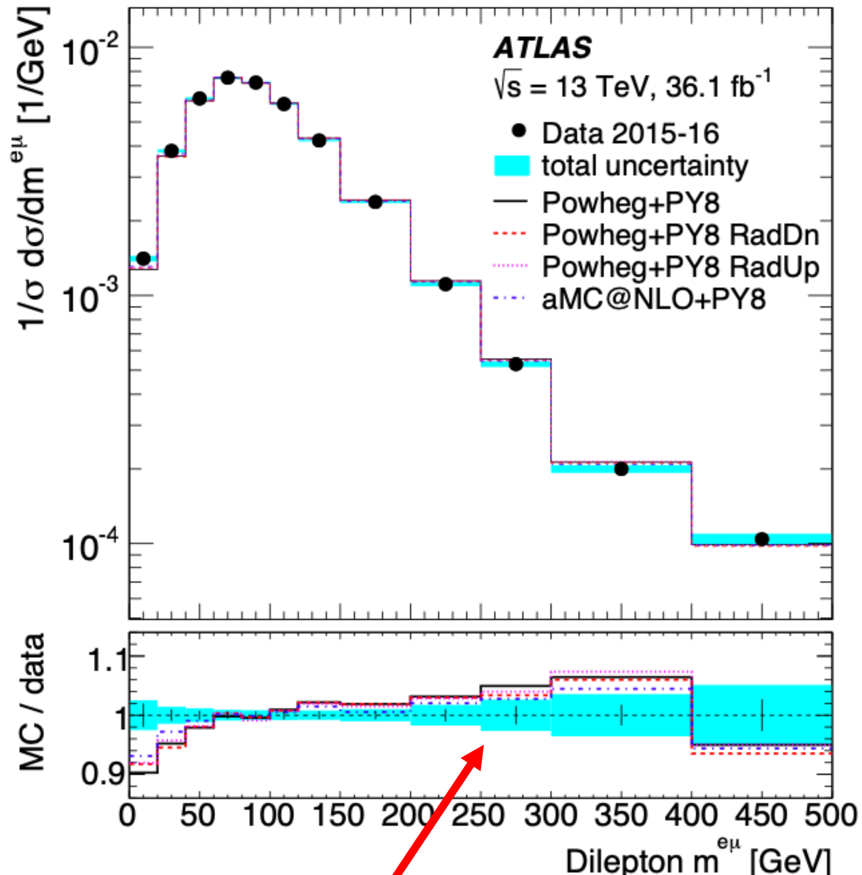

Residual discrepancies at high m_{ll} will be fixed with missing NNLO QCD and NLO EW corrections

Excess at low mll remains prevalent, indicating that effects seen in Run 1 were not statistical fluctuations. Preliminary NNLO QCD corrections do not fix the issue (see Mitov et al.)

V. Ravindran et al.

- F.O. and resummed results for few benchmark values of y

y	LO	LO + LL	NLO	NLO + NLL	NNLO	NNLO + NNLL	NNLO + NNNLL
0.0	4.435 ± 1.145	6.231 ± 1.950	8.255 ± 1.684	9.632 ± 2.286	10.329 ± 1.088	10.938 ± 1.050	10.517 ± 0.820
0.8	4.134 ± 1.067	5.833 ± 1.831	7.517 ± 1.530	8.820 ± 2.124	9.407 ± 0.988	9.992 ± 1.025	9.641 ± 0.718
1.6	3.189 ± 0.819	4.630 ± 1.468	5.522 ± 1.117	6.611 ± 1.676	6.877 ± 0.744	7.380 ± 0.849	7.045 ± 0.563
2.4	1.904 ± 0.492	2.887 ± 0.942	2.985 ± 0.597	$3.715 \pm .998$	3.683 ± 0.410	4.040 ± 0.501	3.821 ± 0.305

Banerjee, Das, Dhani, Ravindran ('17)

- Corrections from LL varies between **40%** to **50%** from LO.
- At NLL it is **17%** to **24%**;
- At NNLL **6%** to **10%**.
- NNLO+NNNLL **3%** to **5%**.

Rapidity distribution is becoming a tool for precision

Scale uncertainty goes down 12% to 6% at NNLO+N3LL

- **The result can be further improved with known NNNLO corrections.**

Ajjath, Chen, Cieri, Das, Gehrmann, Mukherjee, Ravindran (in preparation)

AMS02, PRL 122, 041102 (2019)

Leptophilic excesses, such as positron rise in PAMELA/AMS02